INFORMATION TO USERS

This manuscript has been reproduced from the microfilm master. UMI films the text directly from the original or copy submitted. Thus, some thesis and dissertation copies are in typewriter face, while others may be from any type of computer printer.

The quality of this reproduction is dependent upon the quality of the copy submitted. Broken or indistinct print, colored or poor quality illustrations and photographs, print bleedthrough, substandard margins, and improper alignment can adversely affect reproduction.

In the unlikely event that the author did not send UMI a complete manuscript and there are missing pages, these will be noted. Also, if unauthorized copyright material had to be removed, a note will indicate the deletion.

Oversize materials (e.g., maps, drawings, charts) are reproduced by sectioning the original, beginning at the upper left-hand corner and continuing from left to right in equal sections with small overlaps. Each original is also photographed in one exposure and is included in reduced form at the back of the book.

Photographs included in the original manuscript have been reproduced xerographically in this copy. Higher quality 6" x 9" black and white photographic prints are available for any photographs or illustrations appearing in this copy for an additional charge. Contact UMI directly to order.

UMI

A Bell & Howell Information Company
300 North Zeeb Road, Ann Arbor MI 48106-1346 USA
313/761-4700 800/521-0600

DIFFUSION OF CLASSICAL WAVES IN RANDOM MEDIUM WITH INTERNAL REFLECTION AND MICROSTRUCTURE RESONANCES

by

DMITRY LIVDAN

A dissertation submitted to the Graduate Faculty in Physics in partial fulfillment of the requirements for the degree of the Doctor of Philosophy,

The City University of New York

1996

This manuscript has been read and accepted for the Graduate Faculty in Physics in satisfaction of the dissertation requirement for the degree of Doctor of Philosophy.

1/22/96 — Chair of Examining Committee

Prof. Alexander A. Lisyansky

2/16/96 — Executive Officer

Prof. Joseph Krieger

Prof. Joseph Birman

Prof. Gabriel Cwilich

Prof. Narciso Garcia

Prof. Azriel Genack

Supervisory Committee

The City University of New York

ACKNOWLEDGEMENTS

It really difficult to recognize everyone who helped me in completing my work. The influence of a few individuals is, however, gratefully noted. First, I am personally thankful to my dissertation committee, Drs. Lisyansky, Birman, Cwilich, Garcia and Genack. Special thanks to Drs. Birman and Cwilich who found time to be part of this committee. I wish to express my deepest gratitude to my thesis advisor Dr. Lisyansky. Due to his personal effort my miraculous arrival into the United States became possible. From my first steps in Queens College he always stood by me with encouragement, advise and support. The completion of this thesis would simply never be possible without him. I am deeply thankful for an opportunity to work and learn from him. I would like to express my gratitude to Dr. Genack, numerous discussions with him resulted in a better understanding of waves in random media. His great ideas gave birth to many parts of this thesis and collaboration with his experimental group taught me a lot of valuable things. I am especially thankful to Dr. Garcia who has been advising me since my first days in Graduate school with helpful and valuable words. He was always ready to help with our problems. I would, also, like to thank Dr. Rafanelli who was always able to find the best teaching hours for me. Many thanks to my fellow graduate students without whom life would never be such fun. Very special thanks to Mrs. Susan Wasserman and Mrs. Shierley Allen who never refused to deal with any of my numerous problems. And with additional, and no less special, thanks to the entire physics department where I spent years of learning.

I would also like to thank my wife Svetlana for her dedicated persistence and confidence she had in me. She worked long and hard in helping me to dig this work out of my guts. Without her encouragement, tolerance and help this baby might never have been born. Furthermore, I thank my mother who taught me values in life. I will never forget the sacrifices she made in order to provide me with the necessary things in life. Finally, I would like to thank my best friends Demetrios Iliou who never refused to do anything for me, Philip Braginsky who taught me basics about life in New York and Dmitriy Zaslavskii without whom I would never have learned how to program. It is really a great feeling to know that there is always someone out there that cares for you.

TABLE OF CONTENTS

LIST OF FIGURES

I. INTRODUCTION

The propagation of classical waves is a subject with a long and rich history. We all live in a world occupied by waves. Classical wave propagation in the presence of disorder is the primary subject and indispensable probe in numerous scientific disciplines [1]. The ubiquity of disorder in the Earth's crust, oceans and atmosphere as well as artificial materials makes the propagation of acoustic and electromagnetic waves in a random media a topic of intense scientific and technological interest. Due to the transport of sound, light and microwave radiation through the turbulent atmosphere the wave propagation is a vehicle for communication. It provides a means for discovering structural and dynamical properties of complex systems and may be exploited in novel photonic devices composed of random and periodic dielectric structures. Moreover, classical wave propagation in the presence of disorder serves as a model for quantum transport in mesoscopic systems [2]. On the one hand, the absence of interaction between quanta of classical fields such as occur for electrons simplifies the description of transport. On the other hand, the availability of tunable single frequency sources, short pulses and subwavelength spatial resolution as well as the ability to assemble collections of randomly positioned distinct and movable scatterers make it possible to fully characterize the statistical character of propagation in an ensemble of random samples. Using this broad array of tools it is possible to make detailed measurements of average transport, fluctuations and correlation.

The steady propagation of waves in a random medium can be described by the

ordinary wave equation for a scalar field $\psi(r,t)$ with properties of a medium introduced in the dielectric constant ϵ which in this case is a random function of the coordinate r, $\epsilon = \epsilon(r)$

$$\left\{\nabla^2 + \left(\frac{E}{c}\right)^2 \epsilon(r)\right\} \psi(r,E) = 0; \tag{1.1}$$

where c is the speed of waves in vacuum, $\psi(r,E)$ is a Fourier transform of the $\psi(r,t)$ in the time domain. After formal substitution,

$$\begin{aligned} (E/c)^2 <\epsilon> &= \mathscr{E}, \\ (E/c)^2 [<\epsilon> - \epsilon(r)] &= V(r,\mathscr{E}), \end{aligned} \tag{1.2}$$

where $<\ldots>$ stands for averaging over disorder and $\mathscr{E}$ stands for "energy", Eq. (1.1) resembles the Schrödinger equation for a particle in the energy-dependent potential $V(r,E)$,

$$\nabla^2 \psi(r) + \frac{2m}{\hbar^2}[\mathscr{E} - V(r,\mathscr{E})] = 0 \ . \tag{1.3}$$

Therefore, the same considerations used for Shrödinger particles in a medium with randomly distributed impurities can be in general applied for classical waves.. This opens an unexpected opportunity to apply a number of approaches developed for electronic systems directly to classical waves. The diagrammatic technique developed

for calculation of the electron conductivity and conductance-conductance correlations is one of the most efficient among them in terms of application to classical waves. Electrons, however, are quantum particles satisfying Fermi statistic and their scattering is restricted within the vicinity of the Fermi surface. Although there are no restrictions on scattering of classical waves, results found for classical waves in general replicate those obtained for electrons such as coherent backscattering, correlations in intensity and weak localization. Using the diagrammatic technique, solutions for the amplitude $\langle\psi(\boldsymbol{r})\rangle$ and intensity $\langle|\psi(\boldsymbol{r})|^2\rangle$ of classical waves averaged over disorder are obtained in the form of infinite series which can be conveniently represented by diagrams. Unfortunately, these series can not be summed up explicitly. However, under certain conditions they can be successfully calculated with a good accuracy. One may define a transport *mean free path* ℓ_T, which depends on the properties of the random medium and is regarded as a distance over which the direction of propagation of waves is randomized. When $k_0 \gg \ell_T^{-1}$ (weak scattering regime), where k_0 is a wave vector of the incident wave, the main contribution into series for the intensity of waves comes from "ladder" diagrams which can be summed up exactly. As a result one obtains that the intensity of waves satisfies a diffusion equation with the rate of transport given by the diffusion coefficient,

$$D = \frac{v_E \ell_T}{3} \tag{1.4}$$

where v_E is the transport velocity of waves in the medium.

The solutions of diffusion equation are relatively simple and are available for the

variety of cases. However, some experimental results reveal systematic deviations from theoretical predictions. Experimental data can not be fitted well to theoretical curves in some cases [38,57]. It has been also found that the diffusion constant itself can be a function of the wave vector of the incident wave, that contradicts with conditions of the conventional diffusion theory [38,57]. These discrepancies may be attributed to shortcomings of the initial approximations used in calculations. In general, the random medium is considered to be infinite or semiinfinite. Scatterers are treated as point-like. It leads to a partial loss of the important information about the random medium since in practice all samples are bounded and scatterers are of the finite size often comparable to the wavelength of the incident wave.

Thus, at least two major factors responsible for such discrepancies can be outlined. One of them is internal reflection at the physical boundaries of the random medium, which is present in almost every experiment due to the index mismatch. Because multiple scattering randomizes the wave's direction, a significant fraction of waves attempts to exit at angles exceeding the critical angle. Due to the total internal reflection these waves are reinjected back into the random medium. Waves returning to the random medium are scattered a large number of times within the bulk before they arrive back at the surface where, once again, some of them may be reinjected. Due to many repetitions of this process, waves remain in the medium for substantially longer times than accounted for by diffusion when reflection is ignored. As a result, a diffusion theory ignoring internal reflection may not provide a satisfactory agreement with experimental data.

The second factor that can dramatically affect diffusive transport is an existence of microstructure resonances for classical waves scattering from objects of a size comparable to the wavelength [38-40]. These resonances can be deduced from the exact solution of the problem of electromagnetic wave scattering from a dielectric sphere and are known as Mie resonances [58]. In the vicinity of the principal Mie resonances the value of diffusion coefficient can be low [38]. Thus, the conventional diffusion theory which does not take into account the microstructure of the medium may lead to the erroneous interpretation of experimental data.

In this thesis we provide quantitative description of wave propagation in the bounded random medium with the strong interfacial scattering and microstructure resonances. In the second chapter we develop an approach that describes the steady state diffusive transport. We show, that with proper choice of boundary conditions, diffusion theory is in excellent agreement with optical measurements of the intensity distribution inside the sample and of the intensity profile on the surface of the sample.

Internal reflection from the boundaries not only provides a better agreement between theory and experiment, it may also lead to significant *qualitative* changes in the long range correlations in intensity. Calculations of the long range intensity-intensity correlation function strongly rely on the solution of the diffusion equation and, therefore, it should be affected by internal reflection. In the third chapter of this thesis we derive a general expressions for the spatial and spectral intensity-intensity correlation functions and show that they both exhibit new functional behavior when high reflection from the boundaries is considered.

The effect of microstructure on the diffusion of classical waves is studied in the fourth chapter where we derive the general form of the diffusion coefficient of scalar waves propagating in a resonant random medium. The final expression involves a number of quantities which depend upon properties of individual scatterers. The numerical evaluation of our results is performed in the case when density of scatterers is small. Within this approximation properties of the diffusion coefficient are governed by the off-shell scattering amplitude of a single scatterer, which is calculated for permeable dielectric spheres. We also study the effect of absorption on the diffusion coefficient in this chapter. It is very difficult, sometimes even impossible, to get rid of absorption in any experimental setup. We find that absorption leads to profound changes in the resonant corrections to D. The final section of the chapter is devoted to localization of classical waves.

II. DIFFUSION OF CLASSICAL WAVES IN RANDOM MEDIA WITH REFLECTING BOUNDARIES

2.1 Introduction

It has been recently realized that internal reflection could be very important for different aspects of classical wave propagation in random media. In the paper by Lagendijk *et al.* [4] it was shown that the account for the surface reflection into the diffusion propagator can lead to the better agreement between experiment and theory for the pulse of radiation propagating in the dense random medium. It was also demonstrated by Freund *et al.* [5,6] that by taking into account internal reflection they were able to diminish significantly the discrepancies between their theoretical and experimental results for the optical memory effect. The angular correlation functions in the case of high index mismatch were measured by Zhu *et al.* [8]. They also found, that by including the effect of internal reflection it is possible to obtain agreement between experiment and theory. The role of internal reflection in coherent backscattering was demonstrated by Saulnier and Watson [9].

Usually boundaries of a random medium are considered as perfectly absorbing. However, it is known [1] that the distribution function of diffusive photons is not zero at the boundaries of the sample. Thus, it is incorrect to take zero intensity at the boundaries for diffuse photons inside the medium [1,3]. To resolve this problem an extrapolation

length beyond the boundary in which intensity drops to zero is generally introduced. If this length which is of the order of scattering mean free path $\ell = (n\sigma)^{-1}$ (where n is a density of scatterers and σ is a scattering crossection) for zero boundary reflection, is much less than the thickness of the random media then it can be neglected and the intensity on the boundary can be assumed to be zero. However, the extrapolation length increases with the reflection coefficient $\Re$ [7] and zero boundary conditions can no longer be applied.

In the present chapter we show that with a proper choice of boundary conditions diffusion theory is in an excellent agreement with measurements of the optical intensity profile on the surface of the sample. In the second section the general expression for the intensity of the diffusive waves propagating in the medium with reflecting boundaries is derived. Two different kind of radiation, plane wave and point source, are considered in sections three and four respectively. The time of flight distribution is calculated in the fifth section. And, finally, a comparison with experiment is made in sixth section of this chapter.

2.2 Basic formulas

We consider a steady propagation of the electromagnetic radiation through a slab of a absorbing random medium of infinite extent in the x, y directions situated between $0<z<L$ and whose input and output boundaries have reflection coefficients $\Re^{(in)}$ and $\Re^{(out)}$

respectively. We restrict ourselves to the case of weak scattering, so that the wave interference does not influence average transport. The intensity distribution inside a slab obeys the time independent diffusion equation

$$\nabla^2 I(\boldsymbol{r}) - \alpha^2 I(\boldsymbol{r}) = -\frac{1}{D} Q(\boldsymbol{r}) \tag{2.1}$$

where α is an absorption coefficient $\alpha = (3/\ell\ell_a)^{1/2}$, ℓ_a is an absorption length and $Q(\boldsymbol{r})$ is a source function. In order to solve Eq. (2.1) we need, first, to specify the boundary conditions and, second, to define the source function $Q(\boldsymbol{r})$. We assume that the coherent radiation incident on the sample becomes randomized within a distance z_p, which is of the order of mean free path. We replace the incoming coherent flux by a source of diffusive radiation at the plane $z = z_p$ with a strength equal to the incident flux $Q(\boldsymbol{r}) = Q(x,y)\delta(z-z_p)$ as shown in Fig. 2.1.

Since we made an assumption that there is no incoming diffusive flux through the boundaries, the only flux on the left boundary towards inside of the slab is the reflected part of the flux in the outgoing direction. This gives boundary conditions in the form

$$\begin{aligned} J_+(x,y,z=0^+) &= -\Re^{(in)} J_-(x,y,z=0^+); \\ J_-(x,y,z=L^-) &= -\Re^{(out)} J_+(x,y,z=L^-), \end{aligned} \tag{2.2}$$

where J_+ and J_- are diffusive fluxes in the positive and negative directions respectively.

Using the relationships between the diffusive flux and the intensity of photons [1],

$$J_{\pm}(\boldsymbol{r}) = \frac{I(\boldsymbol{r})\,v}{4} \mp \frac{D}{2}\frac{\partial I(\boldsymbol{r})}{\partial z} \tag{2.3}$$

where v is the speed of the diffusive flux inside the medium, the boundary conditions of Eq. (2.1) can be rewritten as [7,8]

$$\left[\frac{1}{z_0^{(in)}} I(\boldsymbol{r}) - \frac{d}{dz} I(\boldsymbol{r})\right]_{z=0^+} = 0;$$

$$\left[\frac{1}{z_0^{(out)}} I(\boldsymbol{r}) + \frac{d}{dz} I(\boldsymbol{r})\right]_{z=L^-} = 0. \tag{2.4}$$

where

$$z_0^{(in,out)} = \frac{2}{3}\ell\,\frac{1 + \Re^{(in,out)}}{1 - \Re^{(in,out)}} \tag{2.5}$$

In the case of totally reflective boundaries Eqs. (2.4) give the condition that the normal component of the total flux through the boundary is zero. In the case when $\Re^{(in,out)} = 0$ Eqs. (2.4) provide boundary conditions which correspond to perfectly absorbing boundaries.

Let us now assume that the source function has a cylindrical symmetry with respect to the z-axis, i.e., $Q(x,y) = Q(\rho)$, where ρ is the transverse coordinate. Solving

Eq. (2.1) with the boundary conditions given by Eq. (2.4) we obtain for the intensity distribution of the diffusive photons inside the slab

$$I(\rho, z) = \int_0^\infty \frac{d\lambda\,\lambda}{k(\lambda)} J_0(\lambda\rho) \int_0^\infty dx\, x J_0(\lambda x) Q(x) \{ [1 + z_0^{(in)} k(\lambda) z_0^{(out)} k(\lambda)] \sinh[k(\lambda)L] + \quad (2.6)$$

$$k(\lambda)[z_0^{(in)} + z_0^{(out)}] \cosh[k(\lambda)L] \}^{-1} \begin{cases} P_\lambda^{(in)}(z) P_\lambda^{(out)}(L - z_p); & z < z_p \\ P_\lambda^{(in)}(z) P_\lambda^{(out)}(L - z); & z > z_p \end{cases}$$

where $k^2(\lambda) = \lambda^2 + \alpha^2$, $P_\lambda^{(in,out)}(x) = \sinh[k(\lambda)x] + \alpha z_0^{(in,out)} \cosh[k(\lambda)x]$ and $J_0(x)$ is the Bessel function of zero order. Since we are interested in the comparison of our theoretical results with the experimental data we restrict our considerations within two important cases: the first one corresponds to the plane wave incident on the slab and the second one corresponds to the coherent flux focused on the slab surface.

2.3 Plane Wave

The source function in the case of plane wave takes the following form $Q(\rho) = q\nu$, where q is an intensity of a source radiation (see Fig. 2.1), and we obtain a simplified expression for the intensity distribution

$$I(z) = \frac{3q}{\alpha \ell} \left\{ [1 + \alpha^2 z_0^{(in)} z_0^{(out)}] \sinh[\alpha L] + \alpha (z_0^{(in)} + z_0^{(out)}) \cosh[\alpha L] \right\}^{-1} \times \quad (2.7)$$

$$\begin{cases} P_\lambda^{(in)}(z)P_\lambda^{(out)}(L-z_p); & z<z_p \\ P_\lambda^{(in)}(z)P_\lambda^{(out)}(L-z); & z>z_p \end{cases}$$

In obtaining Eq. (2.7) we did not assume the existence of an extrapolation length [7]. However, from the solution (2.7) we can check if extrapolation lengths exist by solving equations

$$I(-z_b^{(in)}) = 0; \qquad I(z_b^{(out)}) = 0. \tag{2.8}$$

One can find that when $\Re^{(in,out)} < \Re_c$, where,

$$\Re_c = \frac{(1 - 2\alpha\ell/3)}{(1 + 2\alpha\ell/3)}, \tag{2.9}$$

Eqs. (8) have solutions,

$$z_b^{(in,out)} = \frac{1}{2\alpha} \ln\left(\frac{1 + \alpha z_0^{(in,out)}}{1 - \alpha z_0^{(in,out)}} \right) \tag{2.10}$$

When $\alpha z_0^{(in,out)} << 1$ we have that $z_b^{(in,out)} \simeq z_0^{(in,out)}$ and for $\Re = 0$ one has $z_0^{(in,out)} = 2\ell/3$, whereas transport theory gives the Milne result, $z_0^{(in,out)} = 0.7104\ell$ [1]. We will incorporate this correction below when finding the transport mean free path from the fit of our theoretical results to the optical measurements. If $\Re^{(in,out)} > \Re_c$ the extrapolation length does not exist since the intensity extrapolated beyond the boundaries never becomes zero. We plot z_b as a function of α in Fig. 2.2.

Using relation (2.10) the expression for the intensity distribution is simplified to the

following form

$$I(z) = I(z_p)\begin{cases} \sinh[\alpha(z+z_b^{(in)})]\Big/\sinh[\alpha(z_p+z_b^{(in)})] & z<z_p \\ \sinh[\alpha(L+z_b^{(out)}-z)]\Big/\sinh[\alpha(L+z_b^{(out)}-z_p)], & z>z_p \end{cases} \tag{2.11}$$

with

$$I(z_p) = \frac{3q}{\alpha\ell}\frac{\sinh[\alpha(z_p+z_b^{(in)})]\sinh[\alpha(L+z_b^{(out)}-z_p)]}{\sinh[\alpha(L+z_b^{(in)}+z_b^{(out)})]} \tag{2.12}$$

The total normalized transmission through the slab can be expressed as,

$$T(L) = \frac{J_{transmitted}(L)}{J_{incident}} = \frac{1-\Re^{(out)}}{qv}J_+(L^-) = \frac{I(L^-)D}{z_0^{(out)}qv} = \frac{1}{\alpha z_0^{(out)}}\frac{\sinh[\alpha(z_p+z_b^{(in)})]\sinh[\alpha z_b(out)]}{\sinh[\alpha(L+z_b^{(in)}+z_b^{(out)})]}. \tag{2.13}$$

In the case of the weak absorption αL, $\alpha z_b^{(in,out)} \ll 1$ Eq. (2.13) reduces to

$$T(L) = \frac{z_b^{(in)}+z_p}{L+z_b^{(in)}+z_b^{(out)}}. \tag{2.14}$$

According to Eq. (2.14) the $T(L)^{-1}$ is directly proportional to the thickness of the slab.

2.4 Point Source

The intensity distribution inside the slab for a point source is defined by Eq. (2.6) with $Q(\rho) = qv\delta(\rho)/\rho$, where qv is a total flux radiating by a source. After some algebra one obtains the following expression for $I(\rho,L)$, necessary for a comparison with experimental results,

$$I(\rho, L) = \frac{q z_0^{(out)}}{D} \int_0^\infty d\lambda\, \lambda\, J_0(\lambda\rho)\, P_\lambda^{(in)}(z_p) \times$$
$$\{ [1 + k(\lambda)^2 z_0^{(in)} z_0^{(out)}] \sinh[k(\lambda)L] + k(\lambda)[z_0^{(in)} + z_0^{(out)}] \cosh[k(\lambda)L] \}^{-1} . \tag{2.15}$$

Integrating the transmitted flux corresponding to the intensity distribution given by Eq. (2.15) leads to the total transmission given by Eq. (2.13).

2.5 Time of flight distribution

The time-dependent photon intensity obeys the diffusion equation which can be written as,

$$\frac{\partial I(\boldsymbol{r},t)}{\partial t} - D\nabla^2 I(\boldsymbol{r},t) + \frac{1}{\tau_a} I(\boldsymbol{r},t) = Q(\boldsymbol{r},t), \tag{2.16}$$

where $\tau_a = \ell_a/c$ is the absorption time and $Q(\boldsymbol{r},t)$ is a source function. We use the same slab geometry as in preceding chapters to solve Eq. (2.16). The boundary conditions for Eq. (2.16), are, therefore, given by Eq. (2.4). Since the index mismatch is the same at the input and output surfaces, we will assume for the sake of simplicity $\Re^{(in)} = \Re^{(out)} =$ and $z_0^{(in)} = z_0^{(out)} = z_0$. To consider photon propagation due to a short pulse injected at $t = 0$ we can take the source function in the form $Q(\boldsymbol{r},t) = qv\delta(\rho)\delta(z-z_p)\delta(t)/\rho$. For $t>0$ the photon intensity can be written as

$$I(\rho,z,t) = qvI_\rho(\rho,t)I_z(z,t)e^{-t/\tau_a}. \tag{2.17}$$

The transverse part, $I_\rho(\rho,t)$, of the intensity can be found to have the following form

$$I_\rho(\rho,t) = \int_0^\infty d\lambda\, \lambda J_0(\lambda\rho)\, e^{-\lambda^2 Dt} \tag{2.18}$$

where $J_0(x)$ is the Bessel function of zero order. The axial part of intensity, $I_z(\rho,t)$, can be found by using the expansion in eigenfunctions

$$I_z(z,t) = \sum_k \psi_k(z_1,t)\,\psi_k(z_2,t)\, e^{-k^2 Dt} \tag{2.19}$$

with $z_1 = z$, $z_2 = L - z_p$ when $z < z_p$ and $z_1 = z_p$, $z_2 = L - z$ when $z > z_p$. Functions ψ_k are given by

$$\psi_k(z) = \left(\sin kx + kz_0 \cos kx\right)\left[\frac{L}{2}(1 + k^2 z^2) + 2z_0\right]^{-1/2} \tag{2.20}$$

with the following equation for the allowed wave numbers

$$\tan(kL) = (2kz_0)/(k^2 z_0^2 - 1). \tag{2.21}$$

The dependence of intensity distributions on the output surface as a function of time for different reflection coefficients is shown on Fig. 2.3.

2.6 Comparison with experiment

We compare Eq. (2.14) with the measurements of $T(L)$ on a slab of 99.7% purity polycrystalline alumina with 0.97 solid fraction. The measurements of total transmission and reflection *vs.* thickness for the sample in air are shown in Fig. 2.4. Within the experimental error of 1% their sum is unity indicating that the sample has level of absorption low enough to assume that the weak absorption approximation is valid. The

inverse of $T(L)$ is plotted in Fig. 2.5. For $L > 100$ μm, $T^{-1}(L)$ is a straight line following the prediction of the diffusion theory in Eq. (2.14). Fitting Eq. (2.14) to the linear portion of the curve gives $z_p = 24.8$ μm and $z_0 = 190.9$ μm with standard deviation σ, respectively, of 0.1 μm and 0.3 μm. The mean free path can only be determined from the measurement of $z_0^{(out)}$ once reflection coefficient is known. To eliminate the internal reflection from the boundaries, the measurements of the relative transmission with sample immersed in index matching fluid were performed [11-13]. These measurements are also shown in Fig.2.5. Although in this case the absolute transmission were not measured, from the x-intercept we obtain $z_0^{(out)} = 22.3 \pm 1.5$ μm. Since $z_0^{(out)} = 0.7104\ell$ in this case, we find $\ell = 31.4 \pm 1.5$ μm.

The prediction of the intensity distribution at the output surface using parameters found in measurements of integrated transmission is an independent test of the adequacy of the diffusion theory. The normalized intensity distribution for different thicknesses in air and index matching fluid is shown in Fig. 2.6. Intensity measurements are shown along a line going through the center of the distribution which is taken as an origin in the figure. For the sample in air we find good agreement with diffusion theory whenever $L > 150$ μm. We would like to stress here that this agreement between theory and experimental data has been achieved *without* using any fitting parameters. Values of all parameters have been taken from measurements of the total transmission. At smaller length scales, however, diffusion fails to describe $I(\rho,L)$ even though measurements of $T(L)$ are in accordance with diffusion theory.

2.7 Conclusion

In conclusion, we have demonstrated that diffusion theory with internal reflection incorporated into the boundary conditions can quantitavely describe a broad array of independent optical measurements of diffusive intensity. These results allow us to determine the mean free path ℓ and penetration length z_p.

III. CORRELATION OF INTENSITY FLUCTUATIONS IN THE PRESENCE OF INTERNAL REFLECTION

3.1 Introduction

The results of the previous chapter indicate that taking account of internal reflection in the diffusion theory leads to an excellent agreement between theory and experiment. In the present chapter we show that the internal reflection may have a notable effect on spatial and spectral intensity-intensity correlation functions. Correlation of classical waves has been subjected to intensive experimental [14-23] and theoretical [23-37] study in the last few years. One of the most important results, obtained by Feng *et al.* [29], is that the intensity-intensity correlation function $C(\boldsymbol{r},\boldsymbol{r}')$ consists, actually, of three parts: short-range C_1, long-range C_2 and "infinite range" C_3. It is established now that the short-range correlation function [14,15,24,31,33] exhibits exponential decay with increasing either separation between points $\Delta r = |\boldsymbol{r} - \boldsymbol{r}'|$ or frequency shift $\Delta E = |E - E'|$. It was shown by Stephen and Cwilich [25] and Pnini and Shapiro [34] that the long-range contribution C_2 also exhibits decay but according to the power-law rather then exponentially. Long-range correlations as a function of wavelength have been observed in the microwave [10,20-22] and optical [19] regions. The C_3 term is found to be somewhat analogous to the constant background [22]. The effect of absorption on long-range correlations was studied in recent papers by Pnini and Shapiro [34] and Kogan and Kaveh

[35]. They found that in agreement with experiments of Genack *et al.* [20] absorption modifies but does not completely destroy long-range correlations in the intensity and these correlations continue to exist even for distances much larger than absorption length. The frequency correlation function in the presence of absorption was also derived by de Boer *et al.* [23] for different incident beam profile.

In recent theoretical studies of the correlation phenomena the Langevin approach proved to be very useful for obtaining long-range spatial and spectral correlation functions. It was first proposed by Zyuzin and Spivak for a study of the conductance fluctuations [27] and then modified for classical waves [28]. This method was later successfully used by a number of authors [23,31,34,35] for photon intensity correlations in random media. According to this approach fluctuating part of the intensity $\delta I = I - \langle I \rangle$ can be found as a solution of the diffusion equation with a random source in the right hand side. In the all above mentioned studies of intensity correlations it was assumed that boundaries are totally absorbing. In this chapter we show that the account for the internal reflection leads to the qualitative changes in the both spatial and spectral correlation functions. These changes occur due to correlations in the waves intensity near the surface of the medium. We show that in the case of low internal reflection the "surface" term becomes negligibly small and we recover previous results [33,34]. In the case of high internal reflection the surface term dominates and we get completely new behavior for both spatial and spectral correlation functions.

3.2 Basic equations

We consider a wave equation for a scalar monochromatic field $\psi(\boldsymbol{r},E)$ of frequency E which is in the presence of absorption is slightly different from Eq. (1.1),

$$\left\{\nabla^2 + k_0^2\,\epsilon(\boldsymbol{r}) + i\frac{k_0}{\ell_a}\right\}\psi(\boldsymbol{r},E) = 0\,, \tag{3.1}$$

$k_0 = E/c$, where c is a speed of wave in the medium free of scatterers, $\epsilon(\boldsymbol{r})$ is the fluctuating part of the refraction index. $\epsilon(\boldsymbol{r})$ is assumed to be a Gaussian random variable with zero mean,

$$\langle\epsilon(\boldsymbol{r})\rangle = 0; \qquad \langle\epsilon(\boldsymbol{r})\,\epsilon(\boldsymbol{r}')\rangle = \epsilon\,\delta(\boldsymbol{r}-\boldsymbol{r}')\,. \tag{3.2}$$

In order to obtain correlations of the intensity $I_E(\boldsymbol{r}) = |\psi(\boldsymbol{r},E)|^2$ we will use Langevin approach. We start our calculations from the Bethe-Salpeter (BS) equation for the field-field correlation function [31],

$$\left\langle\psi(\boldsymbol{r},E)\,\psi^*(\boldsymbol{r}',E')\right\rangle = \left\langle\psi(\boldsymbol{r},E)\right\rangle\left\langle\psi^*(\boldsymbol{r}',E')\right\rangle$$
$$\int d\boldsymbol{r}_1\,d\boldsymbol{r}_2\,d\boldsymbol{r}_3\,d\boldsymbol{r}_4\left\langle G(\boldsymbol{r},\boldsymbol{r}_1;E)\right\rangle\left\langle G^*(\boldsymbol{r}',\boldsymbol{r}_2;E')\right\rangle U(\boldsymbol{r}_1,\boldsymbol{r}_2,\boldsymbol{r}_3,\boldsymbol{r}_4)\left\langle\psi(\boldsymbol{r}_3,E)\,\psi^*(\boldsymbol{r}_4,E')\right\rangle \tag{3.3}$$

where $\langle G \rangle$ is the average Green's function of Eq. (3.1), U is the irreducible four-point vertex function and the integration is taken over the scattering volume occupied by the disordered medium. The function $\langle G(\boldsymbol{r}, \boldsymbol{r}';E)\rangle$ in Eq. (3.3) was calculated for the infinite space by many authors [24,25,31] and has the following form

$$\left\langle G(\boldsymbol{r}, \boldsymbol{r}';E)\right\rangle = \frac{1}{4\pi\,|\boldsymbol{r}-\boldsymbol{r}'|}\exp\left(ik_0\,|\boldsymbol{r}-\boldsymbol{r}'| - |\boldsymbol{r}-\boldsymbol{r}'|/2\tilde{\ell}\right) \tag{3.4}$$

where $\tilde{\ell} = (\ell^{-1} + \ell_a^{-1})^{-1}$. The term $\langle\psi(E)\rangle\langle\psi^*(E')\rangle$ in Eq. (3.3) is exponentially small when both $\boldsymbol{r}$ and $\boldsymbol{r}'$ are taken in the bulk of medium and is usually neglected [23,31]. On the other hand, this term can be considered as a source function $Q_{EE'}(\boldsymbol{r})$ located near the input boundary at the distance of the order of the mean free path. For the weakly scattering regime, in the leading order of the perturbation theory on $(k_0\ell)^{-1}$ the irreducible vertex function $U(\mathbf{r}_1, \mathbf{r}_2, \mathbf{r}_3, \mathbf{r}_4)$ can be taken as

$$U(\boldsymbol{r}_1, \boldsymbol{r}_2, \boldsymbol{r}_3, \boldsymbol{r}_4) = \frac{4\pi}{\ell}\,\delta(\boldsymbol{r}_1 - \boldsymbol{r}_2)\,\delta(\boldsymbol{r}_1 - \boldsymbol{r}_3)\,\delta(\boldsymbol{r}_2 - \boldsymbol{r}_4) \tag{3.5}$$

After this, the Bethe-Salpeter equation (3.3) for the field-field autocorrelation function $\langle I_{EE'}(\boldsymbol{r})\rangle = \langle\psi(\boldsymbol{r},E)\psi^*(\boldsymbol{r},E')\rangle$ can be reduced to the differential equation [31],

$$\nabla^2 I_{EE'}(\boldsymbol{r}) - (\alpha^2 - 2i\beta)\,I_{EE'}(\boldsymbol{r}) = -\frac{1}{D}\,Q_{EE'}(\boldsymbol{r}) \tag{3.6}$$

where $\beta^2 = \omega/2D$ and the frequency shift $\omega = E\text{-}E'$. This equation is valid as long as $\ell/\ell_a \ll 1$ and $\beta\ell \ll 1$, otherwise $\langle I_{EE}(\boldsymbol{r})\rangle$ changes with $\boldsymbol{r}$ too rapidly for the above expansion to hold. If $E' = E$ Eq. (3.6) reduces to the conventional diffusion equation for the photon intensity $\langle I_E(\boldsymbol{r})\rangle$,

$$\nabla^2 \langle I_E(\boldsymbol{r})\rangle - \alpha^2 \langle I_E(\boldsymbol{r})\rangle = -\frac{1}{D} Q(\boldsymbol{r}) \tag{3.7}$$

which is equal to the Eq. (2.1) of the previous chapter. In order to solve Eq. (3.6) one has to specify boundary conditions and the source function. Following the previous chapter we assume that the coherent radiation incident on the slab is effectively randomized in a distance z_p and replace the incoming coherent flux by a source of diffusive radiation at the plane $z = z_p$ with a strength equal to the incident flux. This assumption enables us to use for Eqs. (3.6) and (3.7) the boundary conditions in the form of Eqs. (2.4), developed in the previous chapter. For the sake of the simplicity we consider a *plane wave* incident on the sample surface. In this case, the source function can be written as $Q_{EE}(\boldsymbol{r}) = q\delta(z\text{-}z_p)$, where q is a constant. The solution of Eq. (3.6) can be written in the form,

$$\left\langle I_{EE}(z)\right\rangle = \frac{q}{D} G_\omega(z, z_p) \tag{3.8}$$

where $G_\omega(z,z')$ is a Green's function of the Eq. (3.6) with boundary conditions (2.4),

$$G_{\omega}(z,z') = \frac{1}{a(\omega)}\left[\left(1+a^2(\omega)z_0^2\right)\sinh[a(\omega)L] + 2a(\omega)z_0\cosh[a(\omega)L]\right]^{-1}$$

$$\times\begin{cases} P_{\omega}(z)P_{\omega}(L-z'); & z<z' \\ P_{\omega}(z')P_{\omega}(L-z); & z>z' \end{cases} \tag{3.9}$$

and we defined

$$P_{\omega}(x) = \sinh[a(\omega)x] + a(\omega)z_0\cosh[a(\omega)x];$$
$$a^2(\omega) = \alpha^2 - 2i\beta^2. \tag{3.10}$$

When $\omega = 0$ Eq. (3.10) gives diffusive intensity distribution inside the slab.

3.3 Field-field autocorrelation function

We now consider field-field autocorrelation function $C_1(\omega, z)$ defined as

$$C_1(\omega,z) = \left|\left\langle I_{EE}(z)\right\rangle\right|^2, \tag{3.11}$$

where $\langle I_{EE}(z)\rangle$ is given by Eq. (3.8). The effect of the internal reflection on the autocorrelation function can be easily seen when analyzing Eqs. (3.8,3.9). For low surface

reflection, when $z_0 \sim \ell$ and $z_0\alpha \ll 1$, $z_0\beta \ll 1$ we recover the result, obtained by many authors [23,34,35],

$$C_1(\omega; z>z_p) = \frac{q^2}{c^2} \frac{\cosh[2\gamma_+(L-z)] - \cos[2\gamma_-(L-z)]}{\cosh(2\gamma_+ L) - \cos(2\gamma_- L)}, \tag{3.12}$$

where $\gamma_\pm$ are defined as

$$\gamma_\pm^2 = \frac{1}{2}\left[(\alpha^4 + 4\beta^4)^{1/2} \pm \alpha^2\right]. \tag{3.13}$$

In the absence of absorption, when $\alpha \to 0$, C_1 decays exponentially with respect to the frequency shift ω. However, this behavior changes if reflection becomes large, $z_0\beta \gg 1$. Assuming that conditions $z_p\alpha \ll 1$, $z_p\beta \ll 1$ still hold we obtain,

$$C_1(\omega; z>z_p) = \frac{q^2}{D^2} \frac{\sqrt{\alpha^4+4\beta^4}}{4\beta^4} \frac{\cosh[2\gamma_+(L-z)] + \cos[2\gamma_-(L-z)]}{\cosh(2\gamma_+ L) - \cos(2\gamma_- L)}. \tag{3.14}$$

Due to the prefactor $(\alpha^4+4\beta^4)^{1/2}/\beta^4$, which in the absence of absorption is $(\omega)^{-1}$, autocorrelation function falls-off faster than in the case of small reflection.

3.4 Intensity-intensity long-range correlation function

In this section we consider correlations of the intensity in a tube with a diameter much less than its length L. We may, therefore, consider the correlation function integrated over a crossection of the tube. According to the Langevin approach intensity fluctuations $\delta I = I - \langle I \rangle$ obey the diffusion equation [24,31] with a random source $j_E(z)$ in the right hand side,

$$\left(\nabla - \alpha^2\right)\delta I_E(z) = \frac{1}{D}\nabla \cdot j_E(z)\,. \tag{3.15}$$

The correlator of the random function $j_E(z)$ has the form [34],

$$\langle j_E^{\alpha}(z) j_E^{\beta}(z')\rangle = \delta_{\alpha\beta}\frac{\pi \ell c^2}{3k^2 A}\left|\langle I_{EE}(z)\rangle\right|^2 \delta(z - z')\,, \tag{3.16}$$

where A is a crossection of the tube. In order to solve Eq. (3.15) we apply the same boundary conditions as for Eq. (3.6). The formal solution of Eq. (3.15) can be written in the form

$$\delta I_E(z) = -\frac{1}{D}\left[G_{\omega=0}(z; L) j_E(L) - G_{\omega=0}(z;0) j_E(0)\right] + \frac{1}{D}\int_0^L dz' j_E(z')\frac{d}{dz'}G_{\omega=0}(z; z')\,. \tag{3.17}$$

The first term in this expression which depends upon values taken on the slab surface, is usually neglected [31,34,35]. However, it becomes important when surface reflection is large, so we retain it below. As a result the correlation function splits into two parts: surface $C_{EE'}^{S.T.}$ and volume $C_{EE'}^{V.T.}$ terms,

$$C_{EE'}(z_1;z_2) = C_{EE'}^{S.T.}(z_1;z_2) + C_{EE'}^{V.T.}(z_1;z_2); \tag{3.18a}$$

$$C_{EE'}^{S.T.}(z_1;z_2) = -\frac{1}{D^2}\int_0^L dz'$$

$$\times \left\{ \left[G_{\omega=0}(z_2;L)\frac{dG_{\omega=0}(z_1;z')}{dz'} + G_{\omega=0}(z_1;L)\frac{dG_{\omega=0}(z_2;z')}{dz'} \right] \left\langle j_E(L) j_{E'}(z') \right\rangle \right. \tag{3.18b}$$

$$\left. - \left[G_{\omega=0}(z_1;0)\frac{dG_{\omega=0}(z_2;z')}{dz'} + G_{\omega=0}(z_2;0)\frac{dG_{\omega=0}(z_1;z')}{dz'} \right] \left\langle j_E(0) j_{E'}(z') \right\rangle \right\};$$

$$C_{EE'}^{V.T.}(z_1;z_2) = -\frac{1}{D^2}\int_0^L dz'\,dz''\,\frac{dG_{\omega=0}(z_1;z')}{dz'}\,\frac{dG_{\omega=0}(z_2;z'')}{dz''}\left\langle j_E(z') j_{E'}(z'') \right\rangle. \tag{3.18c}$$

In Eqs. (3.18 b,c) only terms corresponding to the long range correlations are taken into account. Using Eq. (3.9) we finally obtain after some tedious algebra the following

expression for the normalized long-range correlation function,

$$C_2(\omega,R) \equiv \frac{C_{EE}(z_1=L-R;z_2=L)}{\langle I(L)\rangle\langle I(L-R)\rangle} = C_2^{S.T.}(\omega,R) + C_2^{V.T.}(\omega,R); \qquad (3.19)$$

$$C_2^{S.T.}(\omega,R) = \frac{6\pi\alpha z_0^2}{K(\omega)}\left[\frac{P_{\omega=0}(L-R)P_{\omega=0}(L)|P_\omega(z_p)|^2}{P_{\omega=0}(R)} + \alpha z_0|P_\omega(L-z_p)|^2\right]; \qquad (3.20)$$

$$C_2^{V.T.}(\omega;R) = \frac{3\pi}{2K(\omega)}\frac{\alpha^2}{\sqrt{\alpha^4+4\beta^4}}\left\{|P_\omega(L-z_p)|^2\left[I_1(z_p)-J_1(z_p)+I_2(z_p)-J_2(z_p)\right]\right.$$

$$+|P_\omega(z_p)|^2\left[I_3(L-z_p)-I_3(R)-J_3(L-z_p)+J_3(R)+I_4(L-z_p)-I_4(R)-\right. \qquad (3.21)$$

$$\left.\left.J_4(L-z_p)+J_4(R)\right]-\frac{|P_\omega(z_p)|^2P_{\omega=0}(L-R)}{P_{\omega=0}(R)}\left[I_5(R)-J_5(R)+I_6(R)+J_6(R)\right]\right\}.$$

Function $P_\omega(z)$ is defined by Eq. (3.10), the definitions of functions $K(x)$, $I_i(x)$ and $J_i(x)$ are given in Appendix. Since our expression for $C_2(\omega;R)$ is rather complicated for further investigations we consider below important limiting cases for intensity-intensity spectral and spatial correlation functions separately.

3.5 Spatial correlation function

First we consider the spatial correlation function when $\omega = 0$. When absorption is strong, $\alpha L \gg 1$, $\alpha R > 1$ and $\alpha(L - R) > 1$ photons are effectively absorbed inside the slab before reaching the boundary at $z = L$. In this case even large surface reflection should not affect the correlation function. Indeed, we find that the surface term,

$$C^{S.T.}(R) = \frac{6\pi}{k^2 \ell A} \frac{z_0^2}{(z_0 + z_p)^2} \frac{z_0}{(1 + \alpha z_0)^2}; \tag{3.22}$$

is less than the volume term,

$$C^{V.T.}(R) = \frac{3\pi}{4k^2 \ell A}\left(L - R + \frac{3}{4}\alpha^{-1}\right), \qquad \alpha z_0 \ll 1; \tag{3.23}$$

$$C^{V.T.}(R) = \frac{3\pi}{4k^2 \ell A}\left(L - R - \frac{5}{4}\alpha^{-1}\right), \qquad \alpha z_0 \gg 1. \tag{3.24}$$

Eq. (3.23) coincides with the corresponding expression of Refs. [34,35]. The linear decay of $C_2(R)$ in the case of a strong absorption was observed experimentally by Genack et. al. [20]. The dependence of the cross-correlation function upon separation and reflection coefficient is shown in Fig. 3.1. The dependence of C_2 on $\Re$ demonstrates a maximum at $\Re \approx \Re_c$, where $\Re_c$ is defined by Eq. (2.9). This maximum is due to the surface term of the

correlation function. This term, as one can see from Eq. (3.18b) is proportional to the photon flux. The flux is an increasing function of the reflection coefficient for small values of the reflection coefficient and it decreases when reflection coefficient is large. For zero frequency shift it reaches maximum at $\Re_c$. Such a maximum always appears in the dependence of the correlation function upon the reflection coefficient.

In the case of the weak absorption, $\alpha L \ll 1$, $\alpha R \ll 1$, $\alpha z_0 \ll 1$, the correlation function takes the following form,

$$C^{S.T.}(R) = \frac{6\pi}{k^2 \ell A} \frac{z_0^2}{(L+2z_0)^2} \left[\frac{(L+z_0)(L-R+z_0)}{R+z_0} + \frac{(L+z_0-z_p)^2 z_0}{(z_0+z_p)^2} \right]; \qquad (3.25)$$

$$C^{V.T.}(R) = \frac{2\pi}{k^2 \ell A} \frac{1}{(L+2z_0)^2} \left\{ \frac{z_0^3 (L+2z_0)}{R+z_0} \right.$$

$$\left. + (L+z_0-z_p)^2 \left[L+2z_0 - \frac{z_0^3}{(z_p+z_0)^2} \right] - z_0^3 - (L+2z_0)(R+z_0)^2 \right\}. \qquad (3.26)$$

When internal reflection is weak, $z_0 \ll L$, $z_0 < L\text{-}R$, the surface term can be neglected and we obtain the well known result [34,35],

$$C^{V.T.}(R) = \frac{2\pi L}{k^2 \ell A}\left(1 - \frac{R^2}{L^2}\right). \tag{3.27}$$

In the case of strong internal reflection, $z_0 \gg L$, $z_0 \gg R$, the surface term dominates,

$$C^{S.T.}(R) \approx \frac{3\pi z_0}{k^2 \ell A}\left(1 + \frac{L-R}{z_0}\right); \tag{3.28a}$$

$$C^{V.T.}(R) \approx \frac{\pi z_0}{k^2 \ell A}\frac{L-2R}{z_0} \tag{3.28b}$$

and we find a linear falloff of the spatial correlation function. For highly reflecting boundaries, the degree of correlation increases by the factor of $\sim L/z_0$. The crossover from quadratic to linear decay of the spatial correlation function with increasing reflection coefficient can be seen on Fig. 3.2, where we plot C_2 as a function of R and $\Re$. We note that for small reflection $\Re_c \to 1$ and the maximum of the correlation function with respect to $\Re$ appears for very high reflection coefficients.

3.6 Spectral correlation function

We will now consider the spectral correlation function $C_2(\omega;R=0)$. As in the case of the cross-correlation function, for strong absorption, $\alpha L \gg 1$ and $\alpha \gg \beta$, we do not expect a strong dependence upon $\Re$ except for the maximum at $\Re \approx \Re_c$. This dependence is shown in Fig. 3.3. Let us assume that the frequency shift ω is large enough, $\beta \gg \alpha$ and

$\beta L \gg 1$, but limited by the condition $\beta \ell \ll 1$, so that the Eq. (3.6) is valid. In this case, the correlation function has the form,

$$C^{S.T.}(\omega) \approx \frac{3\pi}{k^2 \ell A} \frac{z_0^3}{(z_0 + z_p)^2} \frac{1}{1 + 2\beta z_0 + 2\beta^2 z_0^2}; \tag{3.29a}$$

$$C^{V.T.}(\omega) \approx \frac{3\pi}{k^2 \ell A} \frac{1}{\beta} \frac{1 + \beta z_p z_0^2/(z_0 + z_p)^2}{1 + 2\beta z_0 + 2\beta^2 z_0^2}; \tag{3.29b}$$

Two limiting cases can be distinguished. The first corresponds to small surface reflection when $\beta z_0 \ll 1$. In this case we obtain,

$$C^{S.T.}(\omega) \approx \frac{3\pi}{k^2 \ell A} \frac{z_0^3}{(z_0 + z_p)^2} (1 - 2\beta z_0); \tag{3.30a}$$

$$C^{V.T.}(\omega) \approx \frac{3\pi}{2k^2 \ell A} \frac{1}{\beta} \left[1 - \beta z_0 \frac{z_0^2 + z_0 z_p + z_p^2}{(z_0 + z_p)^2} \right]; \tag{3.30b}$$

The volume term is greater than the surface term by a factor $(\beta z_0)^{-1}$ and the leading term in Eq. (3.30b) gives the well-established result $C_2 \propto (\omega)^{-1/2}$. If we neglect small corrections of the order of βz_0 and βz_p then Eq. (3.30b) coincides exactly with the result first obtained by Pnini and Shapiro [31].

For high surface reflection, $\beta z_0 \gg 1$, however, the frequency dependence changes dramatically,

$$C^{S.T.}(\omega) \approx \frac{3\pi}{2k^2 \ell A} \frac{1}{\beta^2 z_0}\left(1 - \frac{1}{\beta z_0}\right); \tag{3.31a}$$

$$C^{V.T}(\omega) \approx \frac{3\pi z_0}{4k^2 \ell A} \frac{1}{\beta^3 z_0^2}\left(1 - \frac{1}{\beta z_0}\right) \tag{3.31b}$$

and now the surface term dominates again. It, however, decays as $1/\omega$ rather than as $(\omega)^{-1/2}$ as occurs in the case of small reflection. The degree of correlation for small β is $\sim L/z_0$ times greater than in the case of high internal reflection. We plot the autocorrelation function $C_2(\omega;0)$ as a function of the variables ω and $\Re$ in Fig. 3.4.

3.7 Conclusion

In conclusion, we calculated the long-range contribution to the spatial and spectral intensity-intensity correlation functions in the presence of internal reflection. We show that internal reflection can be incorporated into the long range correlation function using proper boundary conditions. We find that in the presence of internal reflection there is an

additional "surface" term in the long range correlation function, in which intensities are taken on the sample surface. When internal reflection is weak this term is small in comparison with "volume" one and our results exactly coincide with already known results. In the presence of strongly reflective boundaries surface term dominates and we obtain qualitatively different dependencies of the correlation functions with respect to a frequency shift and a spatial separation.

IV. DIFFUSION IN PRESENCE OF MICROSTRUCTURE RESONANCES

4.1 Introduction

An important factor that may influence transport properties of classical waves in random media is the presence of microstructure resonances. Usually, random medium is treated as an unbounded collection of randomly distributed point scatterers [2,49,51]. This assumption simplifies calculations greatly allowing one to use conventional perturbative methods in order to describe transport properties of waves. In the case of weak disorder considered in previous chapters one obtains the diffusion equation for the wave intensity with the rate of flow given by the diffusion coefficient defined in Eq. (1.4). Moreover, one finds that v_E is equal to the phase velocity c_p and $\ell_T = \ell/(1-\langle\cos\theta\rangle)$, where θ is a scattering angle. But in practice all scatterers are of particular shape and size. It is well known, that a wave packet scattered from the object of the finite size should spend additional time τ_W on the scattering process itself, in contrast to point scatterers for which this time is equal to zero. The quantity τ_W is called Wigner or dwelling time in the electron theory [52]. Even if τ_W itself is small, one can obtain sizable corrections to the diffusion constant in a medium with a large number of scatterers and this effect is even more significant for classical waves due to, first, an absence of interaction between them and, second, the resonant behavior of their scattering matrix when scatterers are comparable in size to the wavelength. These resonances can be obtained from the solution of the boundary value problem for the electromagnetic wave scattered from the dielectric sphere and are known as Mie resonances

[53]. Recently, it has been suggested by Amsterdam group (AG) [38,39] that these resonances effect the transport velocity v_E, which is no longer equal to the phase velocity in the medium with scatterers of a finite size. They found that in the limit of low density $v_E \approx c_p/[1+n a(k_0)]$ and it depends upon the wave vector of the incident wave k_0. Mie resonances cause strong resonant structure in the correction $a(k_0)$, which leads to the renormalization of the diffusion constant. Analogous corrections to D have also been obtained by Cwilich and Fu [40] and by Kogan and Kaveh [41]. As a result, a conventional expression for D can no longer be applied to describe diffusion in a medium with the scatterers of finite size. It is especially crucial for understanding the nature of the Anderson localization of classical waves [54], at which the usual diffusion becomes impossible and the diffusion constant D=0. The lowering of the diffusion constant due to the resonant contribution shows that considerable care is needed in interpreting the low values of D in studies for the search of classical wave localization. To properly interpret these low values of D all possible sources contributing to its reduction must be calculated from the first principles.

The usual way to obtain the diffusion constant is to look for the asymptotic behavior of the average intensity of the wave $I(\mathbf{q},\omega)$, where $\boldsymbol{q}$ and ω are transferred frequency and momentum respectively [40,42,51]. The function $I(\mathbf{q},\omega)$ satisfies BS equation (the coordinate representation of BS equation is given by Eq. (3.3)) which is a generalized form of the conventional Boltzman kinetic equation. Two approaches have been favorable for further studies of the BS equation. One can solve for D by considering the low-density limit of the BS equation and then expanding in powers of $\boldsymbol{q}$ and ω retaining only the lowest order terms [38-40,42,45]. The alternative approach is the coherent potential approximation

(CPA) used by Kroha *et al.* [43,44] which leads to numerical computations. Despite the similarities in the methods used different results have been obtained. Barabanenkov and Ozrin [42] and independently Kroha *et al.* [43,44] have shown that the transport velocity is not lowered, as it was predicted by the AG, but rather renormalized in the same way as the phase velocity. However, the AG has shown that the conclusion made in Ref. [42], $v_E = c_p + O(n^2)$ where n is the density of scatterers, is due to the omission of the off-shell contribution in the photonic density of states. The proper treatment of the density of states provides the desirable renormalization of v_E.

In the present chapter we use two independent approaches to show that there is another source of the renormalization of D. Microstructure resonances lead not only to the correction to the transport velocity but to the correction to the transport mean free path as well. It is intuitively clear that such a correction to ℓ_T should occur, since Mie resonances provide an additional anisotropy of the scattering matrix and, therefore, should modify $\langle\cos\theta\rangle$. We would like to outline here why these corrections have never been accounted for. The transport mean free path can be found once the diffusion constant and energy velocity are known. As we have already pointed out the diffusion constant can be found from the BS equation where an expansion of all quantities up to the lowest order of q and ω is performed. Then, terms collected near the lowest order of ω provide the correction $a(k_0)$. It has, however, been concluded by AG that all terms in q-expansion cancel after an application of the energy conservation law in the form of the Ward identity (WI). In the present chapter we explicitly show that WI cannot be used for cancellation of terms near the lowest order of q. We identify these terms as a correction to the transport mean free

path.

Another aspect of the calculations of the diffusion constant requires additional attention. Resonant corrections to D involve partial derivatives of the scattering t-matrix for a single scatterer with respect to the wave vector $k = |\boldsymbol{k}|$ and "energy" E. The following procedure of numerical evaluation of the corrections to D, based on the fact that the scattering occurs on shell $k = k_0 = E/c_p$, has been adopted in Refs. [38-40]. The on-shell approximation has been applied to the scattering matrix $t_{\boldsymbol{kk}'}(E)|_{k=E/c} = t(E)$ and then derivatives with respect to E have been taken. As far as derivatives with respect to the wave vector were concerned, it was concluded from the dispersion relation $k^2 = E^2/c_p^2 + nf(k,E)$ that in the limit of low densities $\partial/\partial k \approx c_p \partial/\partial E + O(n)$. These assumptions simplify calculations significantly since the on-shell scattering matrix is simple enough and well known [58]. This approach can, however, lead to incorrect results. The t-matrix for point scatterers, for example, is initially independent of wave vector and, thus, its partial derivatives with respect to wave vector should be equal to zero, whereas the above approach leads to a finite result. Moreover, the functional dependence $t(k)$ is completely different from $t(E)$. The off-shell matrix may also include terms proportional to $(\boldsymbol{k}^2 - E^2)$, which would be zero if the on-shell approximation is applied first and then derivatives with respect to either k or E are taken. If derivatives are taken before the application of the on-shell approximation, the finite result is obtained. Therefore, the off-shell scattering matrix must be used for numerical evaluations.

The effect of absorption on resonant corrections to the diffusion constant is another important issue of the present study. Since in most experiments absorption is rather weak,

it has been usually neglected [38-47]. However, the underestimation of the role of absorption may be misleading. We show, that even weak absorption leads to significant changes in the functional behavior of both corrections. In particular, resonances in the correction $a(k_0)$ drop in magnitude at least 10-25 times.

In the second section of this chapter we derive the most general expression for D with all possible sources of renormalization taken into account. This expression is obtained without employing WI and differs from results obtained by the Amsterdam group [38,39]. The off-shell transfer matrix for a permeable dielectric sphere is derived in the third section of this chapter. A comparison between our correction to the diffusion constant in the off-shell approximation and the results of the Amsterdam group for scalar Mie scatterers employing the on-shell t-matrix is made in the forth section. In the same section we also consider the case of acoustic waves in a hydrodynamic medium. In both cases we find that the functional behavior of our correction to D is different from previously obtained results. In the fifth section of the chapter we consider the effect of absorption on resonant correction to D. We show, that absorption not only causes fundamental alterations in the functional behavior of the diffusion constant but also leads to erroneous results in the case of the on-shell approximation. We find that, for example, within the on-shell approximation absorption can lead to the growth of the diffusion constant which can become larger than its nonresonant value. The final section of this chapter is devoted to the problem of localization of classical waves. We find a new selfconsistency condition on the mobility edge when the appropriate WI for classical waves is applied.

4.2 Derivation of the general expression for D

In order to calculate the diffusion constant it is appropriate to consider the disorder averaged intensity $\langle\psi^2(r,t)\rangle$, with the Fourier transform of the scalar field $\psi(r,t)$ satisfying wave equation (3.1). The field, generated at any point r in space by the point source located at r' can be expressed in terms of the Green function of Eq. (3.1), $\psi(r,t) = G(r,r',t)$. Due to the condition of macroscopic homogeneity the function $|G(r,r',t)|^2$ averaged over disorder has translational invariance, i.e. it depends upon $|r-r'|$ only, and $\langle|G(r,r',t)|^2\rangle$ is a wave intensity $I(r-r',t)$ due to a point source at a point r'. As we have already mentioned, in the weakly scattering regime the space-time Fourier transform of the disorder averaged intensity $I(q,\omega)$ defined as

$$I(q,\omega) = \int_0^\infty dt\, e^{i(\omega+i0)t} \int dR dR' dr dr' \exp[-iq(R-R') - ipr + ip'r']$$

$$\times \left\langle I(q,\omega) = \int_0^\infty dt\, e^{i(\omega+i0)t} \int dR dR' dr dr' \exp[-iq(R-R') - ipr + ip'r' \right.$$

$$\left. \times U(K+\frac{q}{2}, K'+\frac{q}{2}; t)\, U(K-\frac{q}{2}, K'-\frac{q}{2}; t) \right| = \int_{-\infty}^{+\infty} \frac{dE}{2\pi} \sum_{k,k'} \left\langle U_{k_+,k'_+}(E^+) U_{k_-,k'_-}(E^-) \right\rangle \qquad (4.1)$$

$$\equiv \int_{-\infty}^{+\infty} \frac{dE}{2\pi} \sum_{k} \Phi_k(q,\omega;E) = = \int_{-\infty}^{+\infty} \frac{dE}{2\pi} \sum_{k,k'} \Phi_{kk'}(q,\omega;E),$$

where the notations $k_\pm = k \pm q/2$ and $E^\pm = E \pm \omega/2 \pm i0$ were introduced, must have a diffusive pole as $\omega, q \to 0$ (*e.g.*, $I(q,\omega) \propto [-i\omega + Dq^2]^{-1}$). From this pole one can evaluate the diffusion constant. The subject of our primary investigation is, however, not $I(q,\omega)$ but rather the function $\Phi_{kk'}(q,\omega;E)$. On one hand, it inherits all analytical properties of $I(q,\omega)$ including diffusive pole, on the other hand we know an exact form of the equation it satisfies.

It can be shown [55], that the function $\Phi_{kk'}(q,\omega;E)$ is expressed in terms of the Fourier transform of the averaged one-field Green function *via* the Bethe-Salpeter equation

$$\left[-\frac{2E\omega}{c^2}+2q\cdot k\right]\Phi_{kk'}(q,\omega;E)=\Delta G_k(q,\omega)\delta_{k,k'}+\int_{k''}U_{kk''}(q,\omega)\,\Phi_{k''k'}(q,\omega), \qquad (4.2)$$

where

$$G_k(E^{\pm}) \equiv \left\langle G_{k,k'}(E^{\pm})\right\rangle = \delta(k-k')\left[\xi_{\pm}^2-k^2-\Sigma_k(E^{\pm})\right]^{-1} \qquad (4.3)$$

Σ_k is a self energy, and where we denote $\int_k=(2\pi)^{-3}\int dk$, $\Delta G_k(q,\omega;E)\equiv G_{k+}(E^+)-G_{k-}(E^-)$, $\xi_{\pm}=E^{\pm}/c$, $k_{\pm}=k\pm q/2$. A kernel $U_{kk'}(q,\omega)$ has the following form,

$$U_{kk'}(q,\omega) = \Delta G_k(q,\omega)\,K_{kk'}(q,\omega)-\Delta\Sigma_k(q,\omega)\delta_{k,k'} \qquad (4.4)$$

with $\Delta\Sigma_k$ constructed in the manner similar to ΔG_k. The irreducible vertex function $K_{kk'}$ is related to the self energy Σ_k by the generalized Ward identity,

$$-\frac{2\omega E}{c^2}A_k(q,\omega) = \int_{k'}U_{k'k}(q,\omega), \qquad (4.5)$$

with

$$A_k(q,\omega) = \frac{1}{2\xi^2}\left\{\Sigma_{k_+}(E^+) + \Sigma_{k_-}(E^-) + \int_{k'} K_{kk'}(q,\omega)\left[G_{k'_+}(E^+) + G_{k'_-}(E^-)\right]\right\}. \quad (4.6)$$

It is easy to see that for q, $\omega = 0$ Eq. (4.5) reduces to the optical theorem for monochromatic light [63].

In order to solve BS equation for $\Phi_{kk'}$ we will utilize method of eigenfunction expansion developed in Refs. [56,62]. According to this method we look for eigenfunctions $\pi^n_k(q,\omega)$ and eigenvectors $\lambda_n(q,\omega)$ which satisfy the following equation,

$$\left[\frac{2iE}{c^2}\lambda_n(q,\omega) + 2k\cdot q\right]\pi^n_k(q,\omega) = \int_{k'} U_{kk'}(q,\omega)\,\pi^n_{k'}(q,\omega)\,. \quad (4.7)$$

The orthogonality and completeness conditions for π^n_k can be written as,

$$\int_k \frac{\pi^n_k \pi^{n'}_k}{\Delta G_k} = \frac{ic^2}{2E}\delta_{n,n'}; \qquad \sum_n \pi^n_k \pi^n_{k'} = \frac{ic^2 \Delta G_k}{2E}\delta_{k,k'}. \quad (4.8)$$

Since we are looking for a singular part of $\Phi_{kk'}(q,\omega;E)$ we assume that there is a unique eigenfunction π^0_k with an eigenvalue $\lambda_0(q,\omega)$ which behaves as $\lambda_0(q,\omega) \to 0$ when q, $\omega \to 0$. Then we can separate the singular part of $\Phi_{kk'}$ according to

$$\Phi_{kk'}(q,\omega;E) = \frac{\pi^0_k(q,\omega)\,\pi^0_{k'}(q,\omega)}{\lambda_0 - i\omega} + \Phi^{(reg)}_{kk'}(q,\omega), \tag{4.9}$$

with $\Phi_{kk'}{}^{(reg)}$ being finite at q=0, ω=0. Since we are interested in a solution for small q and ω, we can represent both $\pi^0{}_k(q,\omega)$ and $\lambda_0(q,\omega)$ in the form of a Taylor expansion. It immediately follows from Eqs. (4.7) and (4.8) that $\Phi^0{}_k(0,0) = c\mathrm{Im}G_k/(\pi E N_0)^{1/2}$, where $N_0 = \int_k \mathrm{Im}G_k/\pi$ is a density of photonic states and $G_k = G_k(E^-)$. It is now fruitful to apply perturbative methods in order to find corrections to the $\lambda_0(q,\omega)$ and $\pi^0{}_k(q,\omega)$. Taking the deviation $[U_{kk'}(0,\omega) - U_{kk'}(0,0)]$ as a perturbation with the help of Eqs. (4.5) and (4.8) we obtain the first order correction, written for ω→0 in the form

$$\lambda_0(0,\omega) = -i\omega a,$$
$$a = -\frac{1}{\pi N_0}\int_k A_k(0,0)\,\mathrm{Im}G_k. \tag{4.10}$$

Note, that this result is possible only because classical waves obey generalized WI in the form of Eq. (4.5). The usage of the electronic WI would give $U_{kk'}(0,0)=U_{kk'}(0,\omega)$ canceling, therefore, all corrections to the diffusion constant due to the ω expansion. However, the singular behavior of $\Phi_{kk'}(q=0,\omega;E)$ is governed by the correction to the $\lambda_0(0,\omega)$ of the lowest order in q, which can be obtained from Eq. (4.7)

$$\delta\lambda_0(q,\omega) = \frac{c}{\sqrt{\pi E N_0}}\int_k\int_{k'} M_{kk'}(q,0)\,\delta\pi_k^0(q,0) + O(q^2\omega), \tag{4.11}$$

where $M_{kk'}(q,\omega)$ is defined by

$$M_{kk'}(q,\omega) = 2k\cdot q\,\delta_{k,k'} - q\cdot\frac{\partial U_{kk'}(q',\omega)}{\partial q'}\Big|_{q'=0} \tag{4.12}$$

and $\delta\pi_k^0$ is the correction of the first order in $M_{kk'}$ which satisfies the following equation

$$\frac{-2iE}{c^2}\lambda_0(0,\omega)\,\delta\pi_k^0(q,\omega) + \int_{k'} U_{kk'}(0,\omega)\,\delta\pi_{k'}^0(q,\omega) = \int_{k'} M_{kk'}(q,\omega)\,\pi_{k'}^0(0,\omega). \tag{4.13}$$

With the help of the BS equation we can find $\delta\pi_k^0$ as

$$\delta\pi_k^0(q,\omega) = \frac{c}{\sqrt{\pi E N_0}}\int_{k'} M_{kk'}(q,\omega) f_{k'} + O(q\omega). \tag{4.14}$$

where

$$f_k = \lim\int_{k'}\frac{k\cdot k'}{k^2}\Phi_{kk'}(0,\omega;E) - \frac{\partial}{\partial k^2}\mathrm{Re}G_k. \tag{4.15}$$

Our next step is to calculate the term $q\cdot\partial U_{kk'}(q',0)/\partial q'$ which is part of the kernel $M_{kk'}(q,\omega)$. Taking into account that in the case of elastic scattering the quantity $U_{kk'}$ depends only on

the modulus of the wave vectors $|k|^2 = |k'|^2$ and on the cosine of the scattering angle $\mu = k \cdot k'/k^2$ we, first, expand $U_{kk'}(q,0)$ to the first order in q and then take partial derivative with respect to q to obtain

$$q \cdot \frac{\partial U_{kk'}(q',0)}{\partial q'}\Big|_{q'=0} = -2k \cdot q\, \delta_{kk'} \frac{\partial}{\partial k^2} \mathrm{Re}\Sigma_k - \\ - 2k \cdot q\, K_{kk'}(0,0) \frac{\partial}{\partial k^2} \mathrm{Re}G_k - 2iq \cdot (k + k')\, \mathrm{Im}G_k K_1(k,k') . \tag{4.16}$$

In order to calculate the function $K_1(k,k')$ we have to specify exactly the dependence of $K_{kk'}(q,\omega)$ on $k_\pm$ and $k_\pm'$. The expression for $K_1(k,k')$ in the low-density approximation [38,61] is given below by Eq. (4.20). Substitution of Eqs. (4.14) and (4.16) into Eq. (4.11) leads to the singular part of the solution of the BS equation

$$\Phi_{kk'}(q,\omega;E) = -\pi_k(q)\pi_{k'}(q)\,(i\omega - Dq^2)^{-1} \\ \frac{\sqrt{\pi EN}}{c}\pi_k(q) = \mathrm{Im}G_k - \int_{k'} M_{kk'}(q) f_{k'} . \tag{4.17}$$

Here $N=N_0(1+a)$, where a is given by Eq. (4.10), and the diffusion constant is defined as

$$D = \frac{c^2}{3\pi EN}\int_k k^2 f_k \left\{1 + \left[\frac{\partial}{\partial k^2}\mathrm{Re}\Sigma_k + \right.\right.$$

$$\left.\left. \sum_{k'} K_{kk'}(0,0)\frac{\partial}{\partial k'^2}\mathrm{Re}G_{k'} + i\sum_{k'} \mathrm{Im}G_{k'}K_1(k,k')(1+\mu)\right]\right\}. \tag{4.18}$$

Eq. (4.18) represents a general expression for the renormalization of the diffusion constant. In order to obtain the exact expression for D one has to specify how the self-energy Σ_k and irreducible vertex $K_{kk'}$ depend upon the scattering matrix of the individual scatterer.

We evaluate the diffusion constant for the case of the low-density approximation in which the imaginary part of the Green function is sharply peaked at $k = E/c_p$, Im $G_k = \pi\delta(k^2 - E^2/c_p^2)$. Here we defined the phase velocity of light in the random medium as $c_p = c(1-\mathrm{Re}\Sigma_{k0}/E^2)^{-1/2}$. Within the low-density approximation one can also find that the self energy and the irreducible vertex are expressed in terms of the scattering matrix for individual scatterer $t_{kk'}$ and density of scatterers n as $\Sigma^{\pm}(k_{\pm},\omega;E^{\pm})=nt_{k\pm,k'\pm}(E^{\pm})$, $K_{kk'}(q,\omega) = nt_{k+,k'+}(E^{+})t_{k'-,k-}(E^{-})$. Care must be taken to insure that the density of scatterers n is small enough to allow the weak scattering approximation to be valid. After performing the expansion of the self-energy and the vertex into the variables ω and q,

$$\Sigma^{\pm}(k\pm\frac{q}{2},E^{\pm}\pm\frac{\omega}{2}) = nt_{kk}(E^{\pm}) \pm n\frac{\omega}{2}\frac{\partial t_{kk}(E^{\pm})}{\partial E} \pm k\cdot q\frac{\partial t_{kk}(E^{\pm})}{\partial k^2} + O(\omega^2,\omega q,q^2),$$

$$K_{kk'}(q,\omega;E) = n\left|t_{k,k'}(E^{+})\right|^2\left[1 + i\omega\frac{\partial\phi_{k,k'}(E)}{\partial E}\right] + q\cdot(k+k')K_1(k,k') + O(\omega^2,\omega q,q^2). \tag{4.19}$$

we find the following expression for the kernel $K_1(k,k')$

$$K_1(k,k') = in\,\mathrm{Im}\left\{\left[\frac{\partial t_{kk'}}{\partial k^2} + \frac{1-\mu}{k^2}\frac{\partial t_{kk'}}{\partial \mu}\right] t^*_{kk'}\right\}, \tag{4.20}$$

When deriving this equation we denoted the phase shift of the scattering matrix as $\phi_{kk'}(E)$ according to $t_{k,k'}(E^+)=|t_{k,k'}|\exp(i\phi_{kk'})$. Then, after solving BS equation for $\int_{k'} k'\Phi_{kk'}(0,\omega)$ and substituting the result into the expression for f_k, keeping terms in the lowest order of density, we obtain the diffusion coefficient

$$D = \frac{\ell_T c_p}{3(1+na(E))}\left(\frac{c}{c_p}\right)^2\left[1 + n\frac{\partial Re t_{kk}}{\partial k^2} + \frac{inE}{4\pi c_p}\langle(1+\mu)\,K(k,\mu)\rangle_\mu\right]_{k=k_0}, \tag{4.21}$$

where $<...>_\mu$ stands for the averaging over all outgoing wave vectors. Finally, using Eqs. (4.5) and (4.19) we can find the value of a in the low density approximation

$$a(E) = -c^2\frac{\partial}{\partial E^2}\mathrm{Re}t_{kk}(E) + \frac{c}{4\pi}\left\langle |t_{kk'}|^2\frac{\partial\phi_{kk'}(E)}{\partial E}\Big|_{k=k_0=E/c}\right\rangle_\mu + \frac{4\pi c^3}{E}\int_k \mathrm{Im}t_{kk}(E)\frac{\partial}{\partial E^2}\mathrm{Re}G_k(E), \tag{4.22}$$

The value of a was estimated in the low-density approximation by Barabanenkov and Ozrin [42]. They found that $a = (c/c_p)^2 - 1$ and, therefore, concluded that in the low density approximation the diffusion constant is not renormalized. However, this result contradicts

both theoretical calculations [38,39,41] and experimental data [10,23,38]. The Barabanenkov and Ozrin theory was corrected by Lagendijk *et al.* [45]. They have shown that in the vicinity of resonances the shell approximation for $\mathrm{Im}G_k$ used by Barabanenkov and Ozrin is not enough to calculate the quantity a. Thus, their conclusion is that in the vicinity of resonances a is responsible for the renormalization of D.

4.3 An alternative derivation of the diffusion constant in low density limit

In the present section we derive Eq. (4.21) using an independent approach and then analyze it for scalar classical waves. The structure of the BS equation suggests that the function $\Phi_k(q,\omega;E)$ should have isotropic and anisotropic parts. Based on this observation it is convenient to start the solution of the BS equation with the definition of a function

$$P_E(q,\omega) = \sum_k \Phi_k(q,\omega;E)\,, \tag{4.23}$$

which is isotropic and may be regarded as a Fourier transform of the "E-component" of the averaged intensity excited at $\boldsymbol{r}'$ at t=0. The anisotropic properties of the average intensity can be described by the "correlation current" $J_E(q,\omega)$

$$J_E(q,\omega) = \sum_k (k\cdot q)\,\Phi_k(q,\omega;E)\,. \tag{4.24}$$

The next step is to derive a system of equations which would relate these two functions and

then solve for P_E. After integration of Eq. (4.2) and application of the WI in the form of Eq. (4.5) we obtain the continuity equation,

$$-\frac{E\omega}{c^2}P_E + J_E + \frac{E\omega}{c^2}\int_k A_k(q,\omega)\Phi_k(q,\omega) = -\frac{ik_0}{4\pi}\,. \tag{4.25}$$

where we have used that $\int_k \Delta G_k = -\,ik_0/2\pi$. In order to deal with the integral on the left hand side of Eq. (4.25) we can make use of the diffusion approximation ($q \to 0$) and expand $\Phi_k(q,\omega;E)$ to the first order of q

$$\Phi_k(q,\omega;E) \;=\; \Delta G_k(0,0)\left[A_k + (k\cdot q)\,B_k\right]. \tag{4.26}$$

Integration of Eq. (4.26) with respect to k yields the "isotropic" coefficient A_k. Multiplying both sides of Eq. (4.26) by $(k\cdot q)$ and then integrating with respect to k gives the "anisotropic" coefficient B_k

$$\begin{aligned} A_k &= \frac{2\pi i}{k_0}\Delta G_k(0,0)P_E\,; \\ B_k &= \frac{2\pi i}{k_0}\left(\frac{3k\cdot q}{k^2q^2}\right)\Delta G_k(0,0)\,J_E\,. \end{aligned} \tag{4.27}$$

Combining Eqs. (4.26) with Eq. (4.27) gives

$$\Phi_k(q,\omega;E) \;=\; \frac{2\pi i}{k_0}\Delta G_k(0,0)\left\{P_E + \frac{3k\cdot q}{k^2q^2}J_E\right\}. \tag{4.28}$$

Substituting Eq. (4.28) back into Eq. (4.25) and expanding all terms in powers of ω and q

up to the lowest order, we find the continuity equation

$$J_E - \frac{E\omega}{c^2}[1+a(E)]P_E = -\frac{ik_0}{4\pi}. \tag{4.29}$$

where the function $a(E)$ is defined in Eq. (4.10). We now have to derive an equation for the current J_E. We multiply Eq. (4.2) by $\boldsymbol{k}\cdot\boldsymbol{q}$ and integrate it with respect to $\boldsymbol{k}$ using the relation (4.28) to obtain

$$J_E \frac{6\pi i}{k_0}\int_k\int_{k'}\frac{(\boldsymbol{k}\cdot\boldsymbol{q})(\boldsymbol{k}'\cdot\boldsymbol{q})}{k'^2 q^2}U_{kk'}(0,0)\,\Delta G_{k'}(0,0) =$$

$$P_E\left\{\frac{2}{3}k_0^2q^2 - \frac{2\pi i}{k_0}\int_k\int_{k'}(\boldsymbol{k}\cdot\boldsymbol{q})\,U_{kk'}(q,0)\Delta G_{k'}(0,0)\right\}. \tag{4.30}$$

The second term in the right hand side of Eq. (4.30) is important for the calculations of the diffusion constant. It has been concluded by the Amsterdam Group [38,39] and Barabanenkov and Ozrin [42] that after application of the generalized WI in Eq. (4.30) this term is *exactly* equal to zero. If it would have the form $\int_k\int_{k'}(\boldsymbol{k}\cdot\boldsymbol{q})U_{kk'}(q,0)\Delta G_{k'}(q,0)$ the statement made in Refs. [38,39,42] would be correct. It is, however, *impossible* to use WI in the second term of the right hand side of the Eq. (4.30) due to appearance of $\Delta G_k(0,0)$ instead of $\Delta G_k(q,0)$ in it. Instead, one can expand $U_{kk'}(q,0)$ up to the lowest power of q and then solve Eqs. (4.29) and (4.30) for P_E

$$P_E = \frac{c^2}{4\pi c_p[1+a(E)]}\frac{1}{-i\omega+Dq^2}, \tag{4.31}$$

where the diffusion coefficient has the form

$$D = D_0 \left(\frac{c}{c_p} \right)^2 \frac{1 + \Delta(E)}{1 + a(E)}, \tag{4.32}$$

and the bare diffusion constant D_0 is given by

$$D_0 = \frac{1}{3} c_p \left\{ \frac{3\pi}{k_0^2} \int_k \int_{k'} K_{k,k'}(0,0) \Delta G_k(0,0) \Delta G_{k'}(0,0) \frac{(k \cdot q)(k' \cdot q)}{k^2} [1 - \delta_{k,k'}] \right\}^{-1} . \tag{4.33}$$

The expression in curly brackets in Eq. (4.33) represents a conventional transport mean free path ℓ_T. $\Delta(E)$ is an additional correction to the diffusion constant. It can be written as

$$\Delta(E) = -\frac{3\pi i}{k_0} \int_k \int_{k'} \frac{(k \cdot q)}{k_0^2 q^2} \left(\frac{\partial U_{k,k'}(q',0)}{\partial q'} |_{q'=0} \cdot q \right) \Delta G_{k'}(0,0) . \tag{4.34}$$

After taking the partial derivative in Eq. (4.34) and performing integration with respect to k' we find that Eq. (4.32) exactly coincides with Eq. (4.18) of the previous section. It, therefore, proves that Eq. (4.32) represents the most general expression for the diffusion constant of classical waves. The interpretation of the Eq. (4.32) is transparent enough. The diffusion coefficient for any kind of medium and waves can be expressed as $D = v_E \ell / 3$, where ℓ is a general form of a transport mean free path, different from the conventional ℓ_T given by Eq. (4.33). Lagendijk and van Tiggelen [38,39,45,46] have shown that the speed v_E in the case of classical waves is equal to

$$v_E(E) = \frac{c^2}{c_p}\frac{1}{1+a(E)}. \tag{4.35}$$

Than the correction $\Delta(E)$,

$$\ell(E) = \ell_T[\,1+\Delta(E)\,], \tag{4.36}$$

provides a renormalization of the transport of classical waves. Using low density limit in the form of Eqs. (4.19) in Eq. (4.32) we find

$$D = D_0[\,1+(\,\Delta(E)-a(E)\,)\,],$$

$$\Delta(E) = n\frac{\partial \mathrm{Re} t_{k,k}}{\partial k^2} + n\frac{iE}{4\pi c_p}\left\langle (1+\mu)K_1(\boldsymbol{k},\boldsymbol{k}')\right\rangle_{\mu}, \tag{4.37}$$

$$a(E) = n\frac{\partial \mathrm{Re} t_{k,k}}{\partial E^2} - in\sum_{k'}\Delta G_{k'}\left|t_{k,k'}\right|^2\frac{\partial \phi_{k,k'}}{\partial E^2}.$$

In order to compare Eq. (4.37) with previously obtained results the exact expression for the nondiagonal off-shell t-matrix must be known. The details of the calculation of $t_{k,k'}$ for the case of scalar waves are given in the next section.

4.4 Calculation of the off-shell t-matrix

In order to calculate a nondiagonal off-shell transition or t-matrix for a single scatterer we will utilize the general formalism developed in Refs. [59,60]. We introduce the

retarded and advanced Green functions $\mathfrak{S}^{\pm}_{E}(\boldsymbol{r},\boldsymbol{r}')$ for a problem of scattering from a single scatterer that satisfy the differential equations

$$\left[\nabla^2 + \xi_{\pm}^2\right]\mathfrak{S}^{\pm}_{E,outside}(\boldsymbol{r},\boldsymbol{r}') = \delta(\boldsymbol{r}-\boldsymbol{r}') \tag{4.38}$$

outside the single scatterer, and

$$\left[\nabla^2 + M^2\xi_{\pm}^2\right]\mathfrak{S}^{\pm}_{E,inside}(\boldsymbol{r},\boldsymbol{r}') = \delta(\boldsymbol{r}-\boldsymbol{r}') \tag{4.39}$$

inside the scatterer of average index of refraction M. Eqs. (4.38) and (4.39) should be supplemented by boundary conditions that for permeable scatterers have the following form

$$\begin{aligned} &\mathfrak{S}^{\pm}_{E,outside}\big|_{surface} = \mathfrak{S}^{\pm}_{E,inside}\big|_{surface} \;; \\ &\frac{\partial\mathfrak{S}^{\pm}_{E,outside}}{\partial\boldsymbol{r}}\Big|_{surface} = \frac{\partial\mathfrak{S}^{\pm}_{E,inside}}{\partial\boldsymbol{r}}\Big|_{surface} \;. \end{aligned} \tag{4.40}$$

The equation that defines a transition matrix for a single scatterer can be written in a wave-number representation as

$$\mathfrak{S}^{\pm}_{E}(k,k') = \mathfrak{S}^{\pm}_{E,0}(k,k') + \mathfrak{S}^{\pm}_{E,0}(k,k')\,t^{\pm}_{k,k'}(E)\,\mathfrak{S}^{\pm}_{E,0}(k,k') \;. \tag{4.41}$$

with the matrix elements of the free space Green operator $\Im_{E,0}$ given in the wave-number representation by

$$\Im^{\pm}_{E,0}(k,k') = \left[\xi^2_{\pm} - k^2\right]^{-1} \delta(k-k') . \tag{4.42}$$

Then the desired matrix elements are found to be

$$t_{k,k}(E^{\pm}) = [\Im^{\pm}_{E,0}(k)]^{-1} \Im^{\pm}_{E}(k,k') [\Im^{\pm}_{E,0}(k')]^{-1} - \delta(k-k')[\Im^{\pm}_{E,0}(k)]^{-1} . \tag{4.43}$$

In order to calculate the full Green function $\Im_{E}^{\pm}(k,k')$ it is convenient to solve for $\Im_{E}^{\pm}(r,k')$ which satisfies the following differential equations

$$\left[\nabla^2 + \xi^2_{\pm}\right]\Im^{\pm}_{E,outside}(r,k') = e^{ik'r} , \tag{4.44}$$

$$\left[\nabla^2 + M^2\xi^2_{\pm}\right]\Im^{\pm}_{E,inside}(r,k') = e^{ik'r} , \tag{4.45}$$

with the boundary conditions given by Eqs. (4.41) and then perform the Fourier transform with respect to the remaining space variable. For a dielectric sphere of the index of refraction M and radius a one obtains after lengthy but straightforward calculations,

$$t_{k,k'}(E^{\pm}) = \mathfrak{S}^{-1}_{E,0}(k)\frac{4\pi a^2 j_1(|k-k'|)(1-M^2)\xi^2_{\pm}}{|k-k'|(M^2\xi^2_{\pm}-k'^2)} + \mathfrak{S}^{-1}_{E,0}(k)\frac{4\pi a^2(M^2-1)\xi^2_{\pm}}{(M^2\xi^2_{\pm}-k'^2)(M^2\xi^2_{\pm}-k^2)}\times$$

$$\sum_l (2l+1)\frac{j_l'(ka)h_l^{(\mp)}(\xi_{\pm}a) - j_l(ka)h_l^{(\mp)\prime}(\xi_{\pm}a)}{Mj_l'(M\xi_{\pm}a)h_l^{(\mp)}(\xi_{\pm}a) - j_l(M\xi_{\pm}a)h_l^{(\mp)\prime}(\xi_{\pm}a)} P_l(\cos\theta)[M\xi_{\pm}j_{l+1}(M\xi_{\pm}a)j_l(ka) - \tag{4.46}$$

$$kj_l(M\xi_{\pm}a)j_{l+1}(ka)] + \frac{4\pi a^2(M^2-1)\xi^2_{\pm}}{(M^2\xi^2_{\pm}-k'^2)}\sum_l \frac{Mj_l(ka)j_l'(M\xi_{\pm}a) - j_l'(ka)j_l(M\xi_{\pm}a)}{Mj_l'(M\xi_{\pm}a)h_l^{(\mp)}(\xi_{\pm}a) - j_l(M\xi_{\pm}a)h_l^{(\mp)\prime}(\xi_{\pm}a)}\times$$

$$(2l+1)P_l(\cos\theta)[\xi_{\pm}h_{l+1}^{(\mp)}(\xi_{\pm}a)j_l(ka) - kh_l^{(\mp)}(\xi_{\pm}a)j_{l+1}(ka)],$$

where $j_l(x)$ are spherical Bessel functions of the lth order, $h_l^{(+)}(x)$ and $h_l^{(-)}(x)$ are spherical Neumann functions of the first and second kind respectively, $P_l(\mu)$ is the Legendre polynomial of the lth order and $j_l'(x) = d\,j_l(x)/dx$. It worthwhile to mention that when the on-shell limit is used in Eq. (4.46) the well-known result of Ref. [58] for scalar Mie scatterers is obtained.

4.5 Diffusion constant for scalar waves

After performing the angular averaging in Eq. (4.37) we obtain with the help of Eq. (4.46) the expressions for $\Delta(x)$ and $a(x)$ for the case of scalar waves

$$\Delta(x) \equiv -2 - \frac{3}{2x^2}\left\{\sum_{l=0}^{\infty} 4(l+1)^2 \mathrm{Im}\{b_{l+1}^{*}(x)b_l(x)\} - \sum_{l=0}^{\infty}(2l+1)[x\mathrm{Re}b_l(x)\times\right.$$

$$\langle P_l(\mu)(1+\mu)\frac{j_1(2x\sin\theta/2)}{\sin\theta/2}\rangle_{\mu} + \mathrm{Im}B_l(x) + \mathrm{Im}\{B_l^{*}(x)b_l(x)\}] +$$

$$\left.\sum_{l=0}^{\infty}(l+1)\mathrm{Im}\{B_{l+1}(x)b_l^{*}(x) + B_l(x)b_{l+1}^{*}(x)\}\right\}, \tag{4.47}$$

$$a(x) = -1 - \frac{3}{2x^2}\left\{\sum_{l=0}^{\infty}(2l+1)\mathrm{Im}A_l(x) + \frac{3}{x^2}\sum_{l=0}^{\infty}(2l+1)\left[\mathrm{Re}b_l(x)\mathrm{Im}A_l(x) -\right.\right.$$

$$\left.\left.\mathrm{Re}A_l(x)\mathrm{Im}b_l(x)\right] + \frac{3}{x}\sum_{l=0}^{\infty}(2l+1)\mathrm{Re}b_l(x)\langle P_l(\cos\theta)\frac{j_1(2x\sin\theta/2)}{\sin\theta/2}\rangle_{\mu}\right\}.$$

where R is the radius of the scatterer and $x=kR$ is the size parameter. The coefficients A_l and B_l are defined as

$$A_l(x) = \frac{\partial b_l(x,y)}{\partial y}\Big|_{y=x} - ib_l(x)[xh_l^{(-)}(x)j_l(x) + xh_{l+1}^{(-)}(x)j_{l+1}(x) -$$

$$(l+1)h_{l+1}^{(-)}(x)j_l(x) - lh_l^{(-)}(x)j_{l+1}(x)],$$

$$B_l(x) = \frac{\partial b_l(x,y)}{\partial x}\Big|_{y=x} - ib_l(x)[xh_l^{(-)}(x)j_l(x) + xh_{l+1}^{(-)}(x)j_{l+1}(x) - \tag{4.48}$$

$$(l+1)h_l^{(-)}(x)j_{l+1}(x) - lh_{l+1}^{(-)}(x)j_l(x)],$$

The function $b_l(x,y)$ is given by

$$b_l(x,y) = \frac{Mj_l'(My)j_l(x) - j_l(My)j_l'(x)}{Mj_l'(My)h_l^{(\pm)}(y) - j_l(My)h_l^{(\pm)\prime}(y)}, \tag{4.49}$$

and can be recognized as a Van de Hulst coefficient for the TE mode of the vector Mie sphere [58] for $y = x$. Below, we attempt a numerical comparison between Eqs. (4.47-4.49) and the previously obtained results [38,39] for the scattering by scalar Mie spheres. We would like to mention, that our results are also valid for acoustic waves in the hydrodynamic media considered in Ref. [40] for the case when $M = z$, where z is an impedance. Finally, we present calculations of the corrections to D with the on-shell transfer matrix, necessary for the numerical comparison.

The on-shell scattering matrix for the scalar waves can be expressed in terms of the phase shift δ_l in the following form,

$$t_{k,k}(E) = -\frac{2\pi i}{E}\sum_l (2l+1)P_l(\mu)\left[e^{2i\delta_l(E)} - 1\right] = -\frac{2\pi i}{E}\sum_l (2l+1)P_l(\mu)b_l^*(x,x), \tag{4.50}$$

After performing the angular averaging in Eqs. (4.37) we obtain the expressions for $\Delta(x)$ and $a(x)$ for the case of on-shell t-matrix,

$$\Delta(x) \equiv \frac{3}{x^3}\left\{\sum_{l=0}^{\infty} 4(l+1)^2 \sin\delta_l \sin\delta_{l+1} \sin(\delta_{l+1}-\delta_l) - \frac{1}{2}\sum_{l=0}^{\infty}(2l+1)\sin 2\delta_l + x\sum_{l=0}^{\infty}\left[\frac{d\delta_l(x)}{dx}+\frac{d\delta_{l+1}(x)}{dx}\right]\cos^2(\delta_l-\delta_{l+1})\right\}, \tag{4.51}$$

$$a(x) = \frac{3}{2x^3}\left\{x\sum_{l=0}^{\infty}(2l+1)\frac{d\delta_l(x)}{dx} - \frac{1}{2}\sum_{l=0}^{\infty}(2l+1)\sin 2\delta_l\right\}.$$

important for further comparison.

Three corrections to the diffusion constant, $a(x)$, obtained by the Amsterdam group [38,39], $\Delta(x)$ and total correction $\Delta(x)$-$a(x)$, are shown in Figs. 4.1 through 4.3. It is important to point out that Eqs. (4.51) utilizing the on-shell t-matrix has been used in the evaluation of both $a(x)$ [38,39] and $\Delta(x)$ [40], whereas Eqs. (4.47), implementing the off-shell t-matrix, has been employed in the evaluation of our correction. To make a thorough comparison between different corrections, the results in Figs. 4.1- 4.3 have been plotted not only for the same value of $M = 2.73$ (Fig. 4.3) as in the Refs. [38,39], but also for $M =$ 1.5 (Fig. 4.1) and $M = 2$ (Fig. 4.2). The later choice is rather arbitrary and is only based on the fact that for $M > 2$ all three corrections exhibit strongly resonant behavior that makes a detailed comparison between different corrections difficult. On the other hand, one would expect that for values of $M < 2$ Mie resonances to be washed out that can be seen in Fig. 4.1. It is evident from the figures that despite the similarities in the vicinity of the principal Mie resonances at $x \approx 1$, 1.5, 2, 2.5, 3, 3.5, 4 and 4.5, our correction exhibits different functional behavior than previously known. Moreover, the magnitude of our correction for

the principal Mie resonances is much larger than the magnitude of both $a(x)$ and $\Delta(x)$. For example, for the forth Mie resonance located at $x = 2$ ($M = 2.73$) the magnitude of our correction is of the order of 700, whereas the magnitude of $a(x)$ is of the order of 500.

The importance of the off-shell approximation is demonstrated in Figs. 4.4, 4.5 and 4.6 where we have plotted our correction calculated with the help of on-shell (thin line) and off-shell (thick line) t-matricies for the same values of M as in Figs. 4.1-4.3. The changes caused by the off-shell approximation for the transfer matrix are significant for all values of x and for all three indices of refraction. This effect can be attributed to the specific structure of the derivative of $b_l(k,\xi)$ with respect to k involved in $\Delta(x)$ in contrast to $\partial b_l(k,\xi)/\partial\xi$ at constant k involved in $a(x)$. The energy derivative contains differentiation of both numerator and denominator of the Van de Hulst coefficient and, therefore, is proportional to $\partial b_l(x)/\partial x$, which leads to sharp resonances in $a(x)$. The derivative with respect to k involves only the numerator of $b_l(k,\xi)$ and, it can be shown, it is proportional to $b_l(x)$. Magnitudes of the resonances in $b_l(x)$ are much smaller than in $\partial b_l(x)/\partial x$ for $M > 2$ (both terms can be of the same order for $M < 2$) and they are much less sensitive to the value of the index of refraction. In the case of the on-shell approximation, however, $\Delta(x)$ depends on $\partial b_l(x)/\partial x$ and, therefore, exhibits as strong resonances as those of $a(x)$. As a result, the functional behavior of the total correction to D, $a(x) + \Delta(x)$, is significantly altered. Another proof of the importance of the off-shell approximation for the transfer matrix over the on-shell one is given in the next section where resonances in the presence of absorption are considered.

4.6 Resonances in the presence of absorption

In the previous section we have shown that when the microstructure of the medium is taken into account [38-47], the diffusion constant D becomes a function of the wave vector $\boldsymbol{k}$ of an incident wave and it exhibits a strong resonant structure for a wide range of values of k, if scatterers of finite size are considered. The distinctive feature of D as a function of k, worth to be noted here, is that the renormalized diffusion constant is smaller than D_0 for all values of the wave vector. In the present section we study resonant behavior of the diffusion constant when absorption, which can be described by the imaginary part M_i of the complex index of refraction $M = M_r - iM_i$, is present in the medium. We find that the functional dependence of the diffusion constant on k is notably altered by even weak absorption. Moreover, we show that changes in D caused by absorption are very different depending which transfer matrix is used in calculations. In the case of the off-shell approximation we discover that even though absorption changes the structure of the resonances, the value of the renormalized diffusion constant is always less than D_0. This is in agreement with our intuitive understanding of the physics of this phenomena. An application of the on-shell transfer matrix leads to the fundamentally incorrect results. For example, we obtain a noticeable increase in the diffusion constant for scalar classical waves, which may become larger than D_0 for certain values of the wave vector even for very weak absorption. These results, therefore, strongly support the conclusion made in the previous chapter that the off-shell approximation should be used in the evaluation of resonant corrections to the diffusion constant.

The diffusion constant of classical waves propagating in a medium with randomly distributed spherical dielectric (Mie) scatterers of radius R (the value of $R = 1$ cm is used throughout calculations) is given by Eq. (4.37). To speed up calculations it is convenient to express the on-shell renormalization function $a(x)$ in the presence of absorption through the absorption cross section σ_{abs},

$$a(E) = \frac{M_r^2 - 1}{2M_r k_0} \frac{\sigma_{abs}(E)}{M_i} \tag{4.52}$$

rather then use it in the form given by Eqs. (4.51). The case of zero absorption, discussed in Refs. [38,39,41,42], can be obtained from Eqs. (4.52) by taking a limit $M_i \to 0$. We are going to study Eqs. (4.44) together with Eq. (4.48) and (4.49) numerically. The range of values of M_i which can be used in calculations is, however, limited. Eqs. (4.37) for the diffusion constant are obtained within the diffusion approximation which implies that $\ell_T/\ell_a \ll 1$, where $\ell_a = (2M_r M_i k_0)^{-1}$, otherwise the conventional diffusion would break down. As a result, we obtain a condition on M_i written in our conventions as $M_i \ll R/(2M_r \ell_T x)$. The minor inconvenience hidden here is that the transport mean free path itself is a function of a size parameter. Thus, for different values of x we obtain different values of M_i satisfying the validity condition. A possible solution is to use the fact that the scattering mean free path is not changed significantly by absorption and to plot the whole condition $R/(2M_r \ell_T x)$ as a function of x for $M = M_r$ and then use its largest value to find the range of valid values of M_i. In order to be able to make a comparison with previously obtained results [4-7,9] we

use $M_r = 2.73$ in the evaluations. From the plot shown in Fig. 4.7 it is clear that the value of $M_i = 0.005$ would cover the whole range of the size parameter values $0 \le x \le 5$. Our goals are not, however, limited by the plain study of the effect of absorption on resonances. A proof of necessity of the off-shell approximation for the t-matrix is an equally important issue. For this reason we are going to show our results for both approximations.

We plot the on-shell and off-shell versions of the total correction to the diffusion constant, given in the case of low density by $(D-D_0)/D_0 \approx -a(x)+\Delta(x)$, in Figs. 4.8 and 4.9 respectively for the relative index of refraction $M = 2.73 - i0.005$ (thick lines). The figures also show the corresponding correction in the absence of absorption $M = 2.73$ (thin lines). We would like to stress here that we consider very weak absorption and even in this case we find significant changes in the corrections to the diffusion constant. The profound difference between two approximations for t-matrix can be seen from these graphs. The most stricking changes occur in the on-shell correction: it becomes positive at values of the size parameter $x \approx$ 2, 2.5, 3, 3.5, 4, 4.5 and 5, which correspond to the principal Mie resonances. On the other hand, even such weak absorption substantially washes resonances in the off-shell version of the total correction, which, however, remains negative for the whole range of values of the size parameter. In order to understand which correction leads to these changes we will look at properties of $a(x)$ and $\Delta(x)$ separately.

We plot the on-shell version of the correction $a(x)$ in Fig. 4.10 and the off-shell version of $a(x)$ in Fig. 4.11 for $M = 2.73 - i0.005$ (thick lines) and $M = 2.73$ (thin lines). Even weak absorption decreases the magnitude of resonances at least by 10÷25 times. On the other hand the value of $a(x)$ remains positive definite in agreement with the statement of

Ref. [7] that the quantity $k_0^2 a(E)$ represents positive definite "potential energy" inside the scatterers.

The effect of absorption on the on-shell (Fig. 4.12) and off-shell (Fig. 4.13) versions of the correction $\Delta(x)$ is different. A special attention has to be paid to the off-shell version of $\Delta(x)$ in the absence of absorption. It is positive for the wide range of values of x, thus leading to the growth of the transport mean free path. These changes occur in the vicinity of the first five principal Mie resonances located at values of $x \approx 1$, 1.5, 2, 2.5 and 3. These peculiarities can be understood if we look at properties of Mie resonances. The transport mean free path given by Eq. (4.33) can be rewritten in its traditional form $\ell_T = \ell/(1-\langle\mu\rangle)$. It is known that in the vicinity of principal Mie resonances scattering is primarily in the forward direction [58]. Thus, the average cosine of the scattering angle increases leading, therefore, to the growth of the transport mean free path. Analogous features can not be found in the on-shell version of $\Delta(x)$. It is always negative and it basically replicates features of $a(x)$ shown by a thin line in Fig. 4.10. When absorption is introduced in the medium, resonances are washed out in the case of the off-shell version of $\Delta(x)$, which becomes now negative for values of $x = 2.5$ and 3. The functional behavior of the on-shell version of $\Delta(x)$ is altered much more seriously. It becomes positive due to inversion of the principal Mie resonances that is shown in Fig. 4.12, while the rest of it is hardly affected by absorption.

Let us return to the total correction to the diffusion constant. In the on-shell approximation absorption "stimulates" diffusion since the renormalized value of D becomes greater than D_0. This result, however, can be hardly justified physically. Contrary, the

growth of the transport mean free path in the case of the off-shell t-matrix is not strong enough to stimulate diffusion in the medium, since $\Delta(x)$ is always less than $a(x)$. Even in the presence of absorption, when $a(x)$ is strongly decreased, $\Delta(x)$ is decreased as well, thus keeping the total correction to D negative. It, therefore, supports our suggestion that it is incorrect to use the on-shell t-matrix in the evaluation of the diffusion constant.

We can summarize here that absorption leads to serious changes in the resonant corrections to the diffusion constant. In addition, we show that an application of the on-shell transfer matrix to resonances can lead to erroneous results. It is shown in the present section that one of these results is the possible growth of the diffusion constant in the presence of absorption. It signifies the fundamental importance of the off-shell approximation for the evaluation of the resonant corrections to the diffusion constant.

4.7 Correction to selfconsistent theory of localization of classical waves

In the present section we study the effect of microstructure on the weak localization of classical waves. The mechanism responsible for this phenomenon is the constructive interference in the backscattering direction between the wave following one of the scattering paths and another wave following the time-reversed path. It results in a higher probability for the wave to be scattered in the backward direction effectively reducing the diffusion constant. The mathematical formalism of this effect for electrons developed by Vollhard and Wolfe [47] has been later applied for classical waves by many authors [48-51].

It was suggested, that in the presence of time-reversed symmetry the Boltzman approximation for BS equation is an oversimplification. According to this approximation, the irreducible vertex $K_{kk'}$ in the BS equation which describes wave coupling can be represented by a series of so-called "ladder" diagrams. To include more terms in $K_{kk'}$, Vollhard and Wolfe identified "maximally crossed" diagrams as the dominant higher order contribution to the irreducible vertex that also correspond physically to the coherent backscattering effect. It has been already discussed in the Introduction that considerations used for Shrödinger particles can be in general applied for classical waves. As a result, the condition for calculating localization phase diagrams can be obtained and scaling behavior near the mobility edge can be studied. However, in all previous studies the application of the electronic theory of weak localization was extended too far for classical waves, when electronic WI was directly applied for them. The WI for classical waves is different. Upon substitution into the BS equation it leads to additional renormalization of the diffusion constant. In the present section we intend to apply this approach to the problem of weak localization of classical waves.

As we have mentioned, in order to study the diffusion constant in the vicinity of the localization transition we have to substitute in the Eqs. (4.32-34) the following form of the four point vertex

$$K_{kk'}(q,\omega) = K^{B}_{kk'}(q,\omega) + K^{M}_{kk'}(q,\omega)\,, \qquad (4.53)$$

where the Boltzman part $K_{kk'}^{B}(q,\omega)$ is the result of the summation of the "ladder" diagrams and the contribution of the "maximally crossed" diagrams is represented by $K_{kk'}^{M}(q,\omega)$. A major disadvantage of the expression for D in the form of Eq. (4.32) is that it involves partial derivatives of $K_{kk'}^{M}$ with respect k which can be hardly evaluated analytically. The diffusion coefficient can, however, be successfully modified to the form without derivatives of the four point vertex. For this purpose we shall use the same procedure as in the third section of this chapter. Our primary goal is to obtain an equation for the current J_E different from Eq. (4.30). We start from the alternative form of the BS equation

$$\Phi_k(q,\omega;E) = G_{k_+}(q,\omega)G_{k_-}(q,\omega) + G_{k_+}(q,\omega)G_{k_-}(q,\omega)\int_{k'} K_{kk'}(q,\omega)\Phi_{k'}(q,\omega;E) \,. \quad (4.54)$$

Next, we multiply Eq. (4.54) by the factor $(k\cdot q)$ and integrate it with respect to k while using Eq. (4.28) to obtain

$$J_E\left\{1 - \frac{2\pi i}{k_0}\int_k\int_{k'} \frac{k\cdot k'}{k'^2}|G_k(0,0)|^2 K_{kk'}(0,0)\Delta G_{k'}(0,0)\right\} =$$

$$\frac{4\pi i}{3}q^2 k_0 P_E\left\{\int_k \frac{k^2}{2k_0^2}\left[\Delta G_k^2(0,0) + (G_k^+(0,0))^2\frac{\partial\Sigma_k^+(0,0)}{\partial k^2} + (G_k^-(0,0))^2\frac{\partial\Sigma_k^-(0,0)}{\partial k^2}\right] - \right. \quad (4.55)$$

$$\left.\int_k\int_{k'} \frac{k\cdot k'}{k^2}|G_k(0,0)|^2 K_{kk'}(0,0)\frac{\partial \mathrm{Re}G_k(0,0)}{\partial k^2}\right\}.$$

We solve Eqs. (4.29) and (4.55) for P_E and, therefore, for D

$$D(E) = \frac{k_0 c^2}{3c_p(1+a(E))} \frac{\int_k \frac{k^2}{2k_0^2}\Delta G_k^2(0,0) + B(E)}{\frac{k_0}{4\pi} - \Phi(E)},$$

$$B(E) = \int_k \mathrm{Re}(G_k^2(0,0)\frac{\partial \Sigma_k(0,0)}{\partial k^2}) + \int_k \int_{k'} \frac{k\cdot k'}{k^2} |G_k(0,0)|^2 K_{kk}(0,0) \frac{\partial \mathrm{Re}G_k(0,0)}{\partial k^2}, \tag{4.56}$$

$$\Phi(E) = \int_k \int_{k'} \frac{k\cdot k'}{k'^2} |G_k(0,0)|^2 K_{kk'}(0,0)\, \mathrm{Im}G_{k'}(0,0) .$$

The presence of the term $B(E)$ in the numerator of Eq. (4.56) is completely due to the application of the WI for classical waves. We shall perform evaluations in Eq. (4.56) using the Lloyd model [64] which presumes that the self energy is independent of the momentum. To proceed further, let us define a complex $k^* = \Delta k + i / 2\ell$ such that

$$G_k(0,0) = \frac{1}{(k^*)^2 - k^2} = \frac{1}{k_0^2 - k^2 - \Sigma_k} . \tag{4.57}$$

Eq. (4.57) leads to the following relations

$$\mathrm{Re}(k^*)^2 = \Delta k^2 - \frac{1}{4\ell^2} = k_0^2 - \mathrm{Re}\Sigma_k ;$$

$$\mathrm{Im}(k^*)^2 = \frac{\Delta k}{\ell} = -\mathrm{Im}\Sigma_k . \tag{4.58}$$

In the previous sections of the present chapter we have used that $\Delta k\ell \gg 1$. Under this condition $\Delta k^2 \cong (k^*)^2 = k_0^2 - \mathrm{Re}\Sigma_k$ and we have been able to apply the on-shell approximation for $\Delta G_k(0,0)$. However, the possibility that $\Delta k\ell \cong 1$ is now to be taken into account. Under this condition $\Delta G_k(0,0)$ takes the form

$$\Delta G_k(0,0) = \frac{-2i\gamma\ell^2}{(\gamma^2 - 1/4 - k^2\ell^2)^2 + \gamma^2}, \tag{4.59}$$

where $\gamma = \Delta k\ell$. The contribution into the four point vertex due to the summation of the maximally crossed diagrams can be found to have the following form in our notations

$$K^M_{kk'}(0,0) = \frac{\gamma^2 c_p}{2\pi^2 k_0^2 \ell^4} \frac{1}{D^B(E)\,|k+k'|^2}. \tag{4.60}$$

where the diffusion constant in the Boltzman representation $D^B(E)$ is given by Eq. (4.32). An important step allowing one to extend the Green function formalism from the weak scattering regime to the regime of strong scattering is to replace $D^B(E)$ in the Eq. (4.60) by the renormalized diffusion constant, $D(E)$

$$K^M_{kk'}(0,0) = \frac{\gamma^2 c_p}{2\pi^2 k_0^2 \ell^4} \frac{1}{D(E)\,|k+k'|^2}. \tag{4.61}$$

This has the effect of making the theory selfconsistent as first proposed by Vollhard and Wolffle [55]. Performing integrations in Eqs. (4.56) with the help of Eqs. (4.59, 61) and $K_{kk'}{}^{B}$ given in previous chapter we obtain the self-consistency equation for the diffusion coefficient

$$D(E) = D^{B}(E)\frac{1}{1+\frac{c^2}{c_p^2}a^{M}(E)}\frac{1+\frac{4\pi\gamma\ell_T c_p}{3k_0\ell^2 D^{B}}\Phi^{M}(E)}{1-\frac{2\pi\gamma\ell_T}{k_0^2\ell^2}B^{M}(E)}, \tag{4.62}$$

with

$$\begin{aligned} a^{M}(E) &= \frac{c_p\gamma^2\Delta k_c}{2\pi k_0^4\ell^2(\gamma^2-1/4)D(E)}, \\ \Phi^{M}(E) &= \frac{c_p\Delta k_c\ell(\gamma^2-1/4)^{1/2}}{4\pi^2 k_0^2\gamma D(E)}, \\ B^{M}(E) &= -\frac{c_p\Delta k_c(\gamma^2-1/4)^{1/2}}{2k_0^2\ell D(E)}, \end{aligned} \tag{4.63}$$

where Δk_c is a cutoff momentum. In the vicinity of the localization transition where D tends to go to zero value the selfconsistency equation takes the form

$$\frac{3\pi}{2}\frac{\gamma^3(E_c)\Delta k_c}{k_0^7\ell^6} = 1. \tag{4.64}$$

Here E_c stands for the mobility edge. The presence of γ^3 in the numerator of Eq. (4.60) makes it different from previously known results [47-51] where the first power of γ was obtained in the selfconsistency equation. The latter is wholly due to an application of the correct WI for classical waves in calculations of the diffusion coefficient.

4.8 Conclusion

In conclusion we have calculated the general expression for the renormalization of the diffusion coefficient for classical waves propagating in the random medium with microstructural resonances. The low density limit together with off-shell approximation for a scattering t-matrix have been applied for estimations of the diffusion constant. We find that the functional behavior of the renormalization terms is altered comparing to results obtained by other authors where the on-shell matrix was implemented. An important question is a possible comparison of the obtained results with experimental data (see, for example, Ref. 57). However, the comparison of our results with an experiment is limited by the low-density approximation used in calculations. When propagation occurs in a medium with a high relative index of refraction both renormalization terms can become very large (see Figs. 4.7 and 4.8) thus requiring low enough densities to provide the condition $|D - D_0|/D_0 \ll 1$ to insure the applicability of the low-density approximation. However, the filling fractions used in experiment range from 15% to 35% that are not enough to satisfy the low density approximation in the vicinity of resonances. Thus, the Eq. (4.32) cannot be used for the direct comparison between theory and experiment that is possible only if the

account for higher powers in density of scatterers is made. We also observe that the functional behavior of the diffusion constant on the wave vector changes in the presence of absorption. Moreover, absorption leads to the growth of the total correction to D when the on-shell transfer matrix is used in evaluations. This erroneous result proves that the off-shell t-matrix should be used in calculations. Finally, we discuss corrections to the selfconsistent theory of localization of classical waves arising due to the application of the correct WI for classical waves. We find new selfconsistensy condition for the mobility edge of classical waves.

V. SUMMARY

In this thesis, we have presented a theoretical description of the propagation of classical waves in random medium. An emphasis has been made on developing theoretical approaches to the random media as close as possible to real systems. In order to achieve this goal, we incorporated interfacial scattering into the diffusion model and investigated the effect of the microstructure on the transport parameters of waves propagating in the medium with and without absorption. We have demonstrated that the internal reflection from the sample's boundaries is important for providing good quantitative agreement between theory and experiment. Furthermore, we have shown that the diffusion theory with internal reflection incorporated into the boundary conditions can quantitatively describe a broad array of independent optical and microwave measurements including total transmission, surface intensity profiles and transit time distributions. These results allow us to determine transport mean free path ℓ. The account for internal reflection from the boundaries not only leads to a better agreement between the theory and experiment. Strong reflection from the boundaries of the sample can lead to significant changes in the such fundamental quantity underlying wave propagation in the random medium as long-range correlations in intensity. In this thesis, the long-range contribution to the spatial and spectral intensity-intensity correlation functions in the presence of internal reflection is calculated. An additional "surface" term in the long range correlation function, in which intensities are taken on the sample surface, is found. In the case of weak reflection from the boundaries this term is

small in comparison with known "volume" one and our results exactly coincide with already known results. In the presence of strongly reflective boundaries the surface term dominates and we obtain qualitatively different dependencies of the correlation functions with respect to a frequency shift and a spatial separation.

The effect of the microstructure of the random medium and absorption on transport parameters of classical waves including diffusion constant and transport mean free path is also considered. The general expression for the renormalization of the diffusion coefficient for classical waves propagating in the random medium with scatterers of finite size is calculated. This result is valid for scatterers of any shape and size. The diffusion constant is estimated in the low density limit for scalar waves scattered by dielectric spheres. The off-shell scattering matrix required for calculations is obtained for permeable Mie spheres. The renormalization terms show a resonant structure with the functional behavior significantly different from the results obtained by other authors where the on-shell matrix was implemented. The importance of the off-shell approximation for the evaluation of the diffusion constant is demonstrated. Such drawback of the theory as the low density limit does not, however, allow a detailed comparison between theory and experiment. We also show, that absorption may have a surprisingly strong impact on the diffusion constant of scalar classical waves which may become greater than its classical value $D = c\ell_t/3$. We relate this effect to the increasing of the resonant correction to the transport mean free path in the presence of absorption.

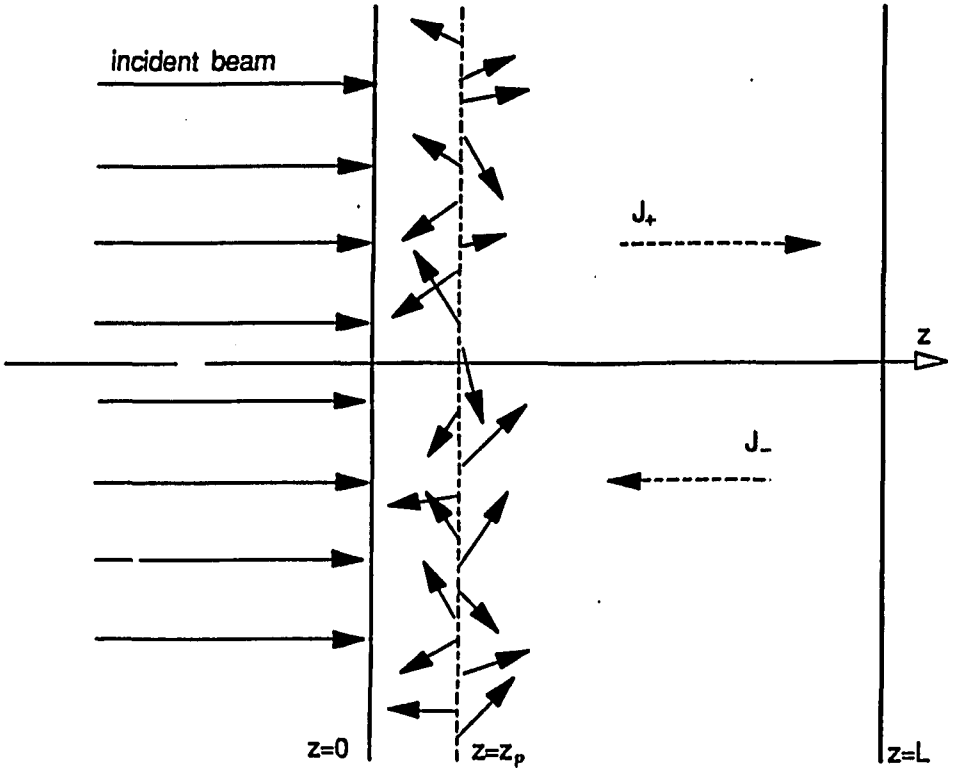

Figure 2.1

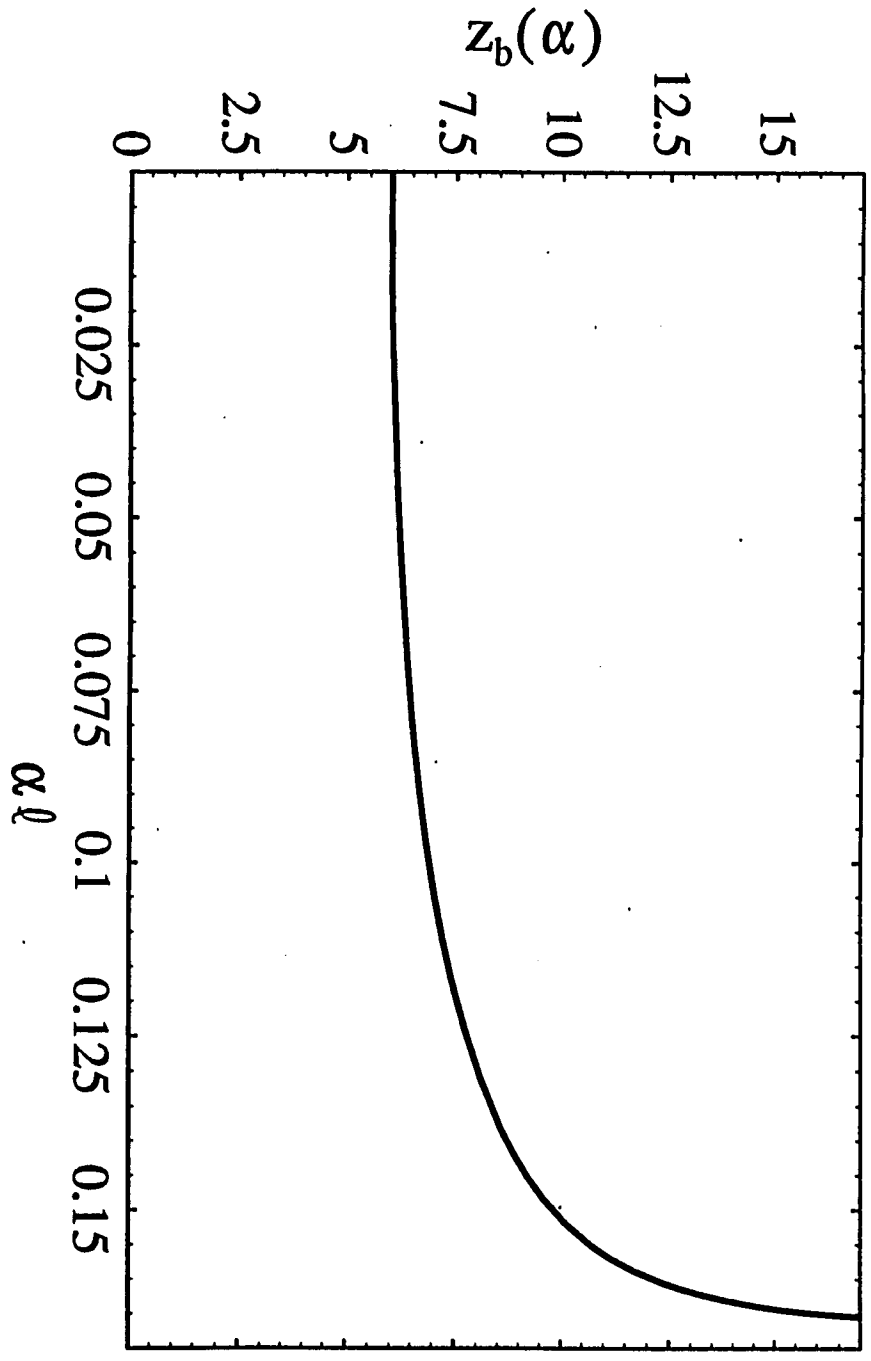

Figure 2.2

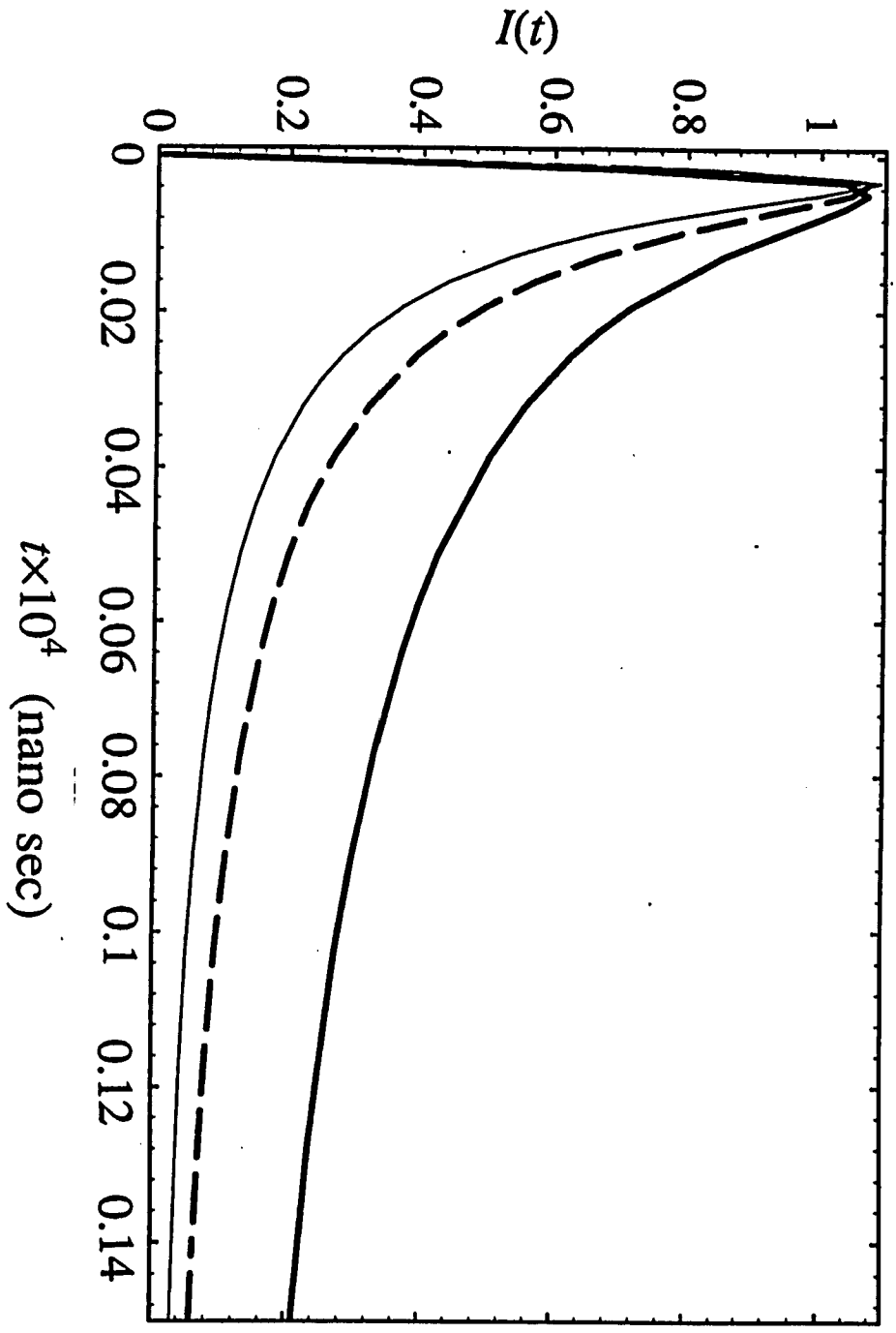

Figure 2.3

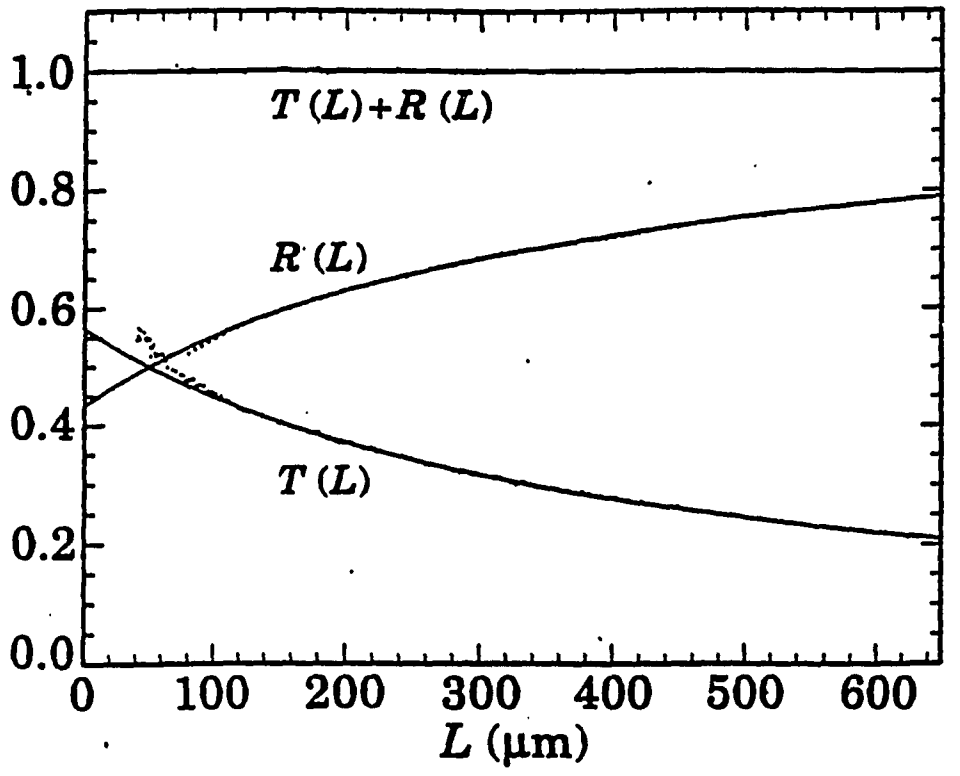

Figure 2.4

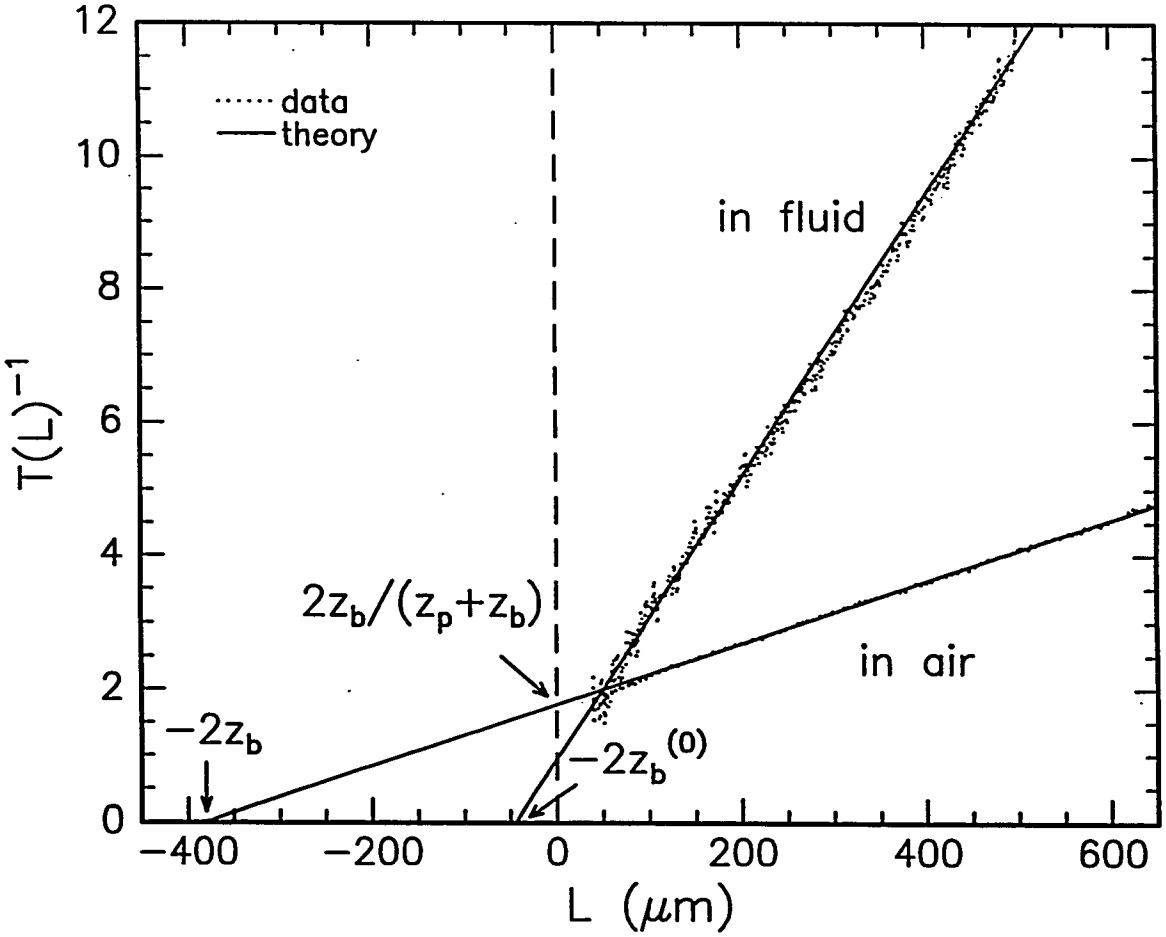
12
10
8
6
4
2
0
T(L)$^{-1}$
data
theory
in fluid
in air
$2z_b/(z_p+z_b)$
$-2z_b$
$-2z_b^{(0)}$
−400
−200
0
200
400
600
L (μm)

Figure 2.5

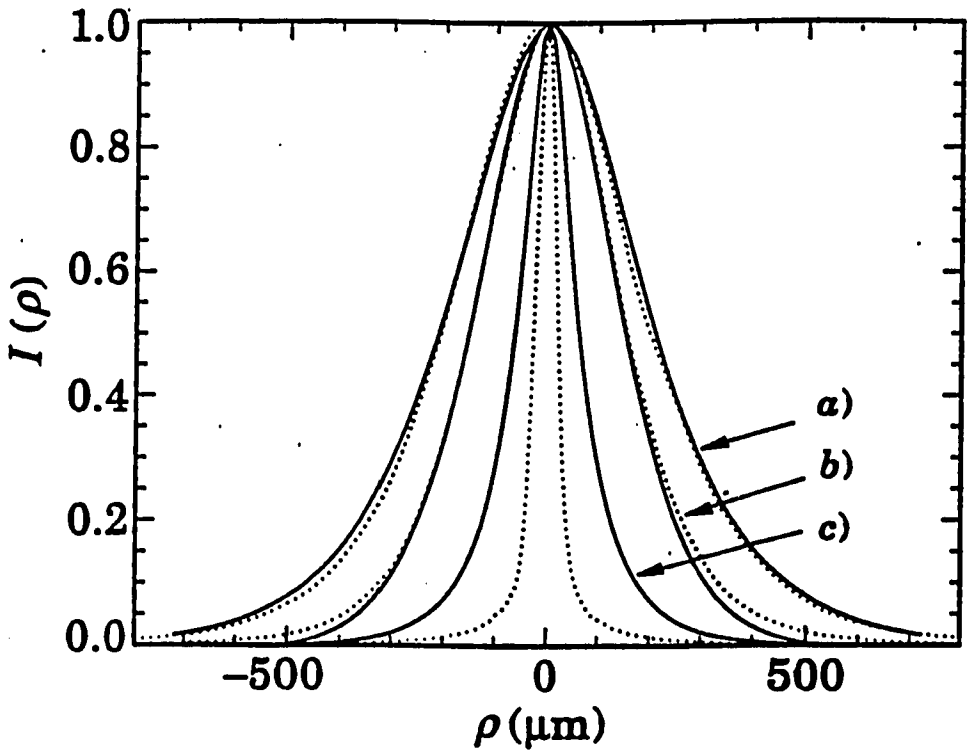

Figure 2.6

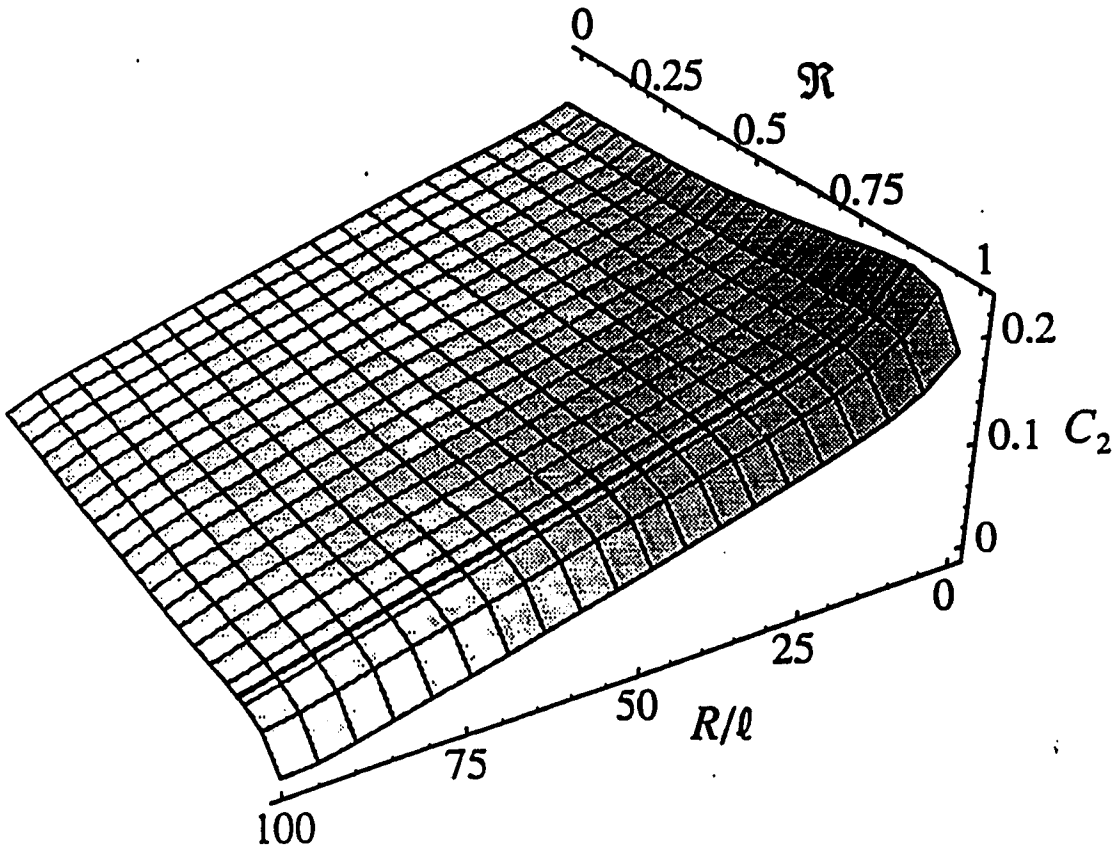

Figure 3.1

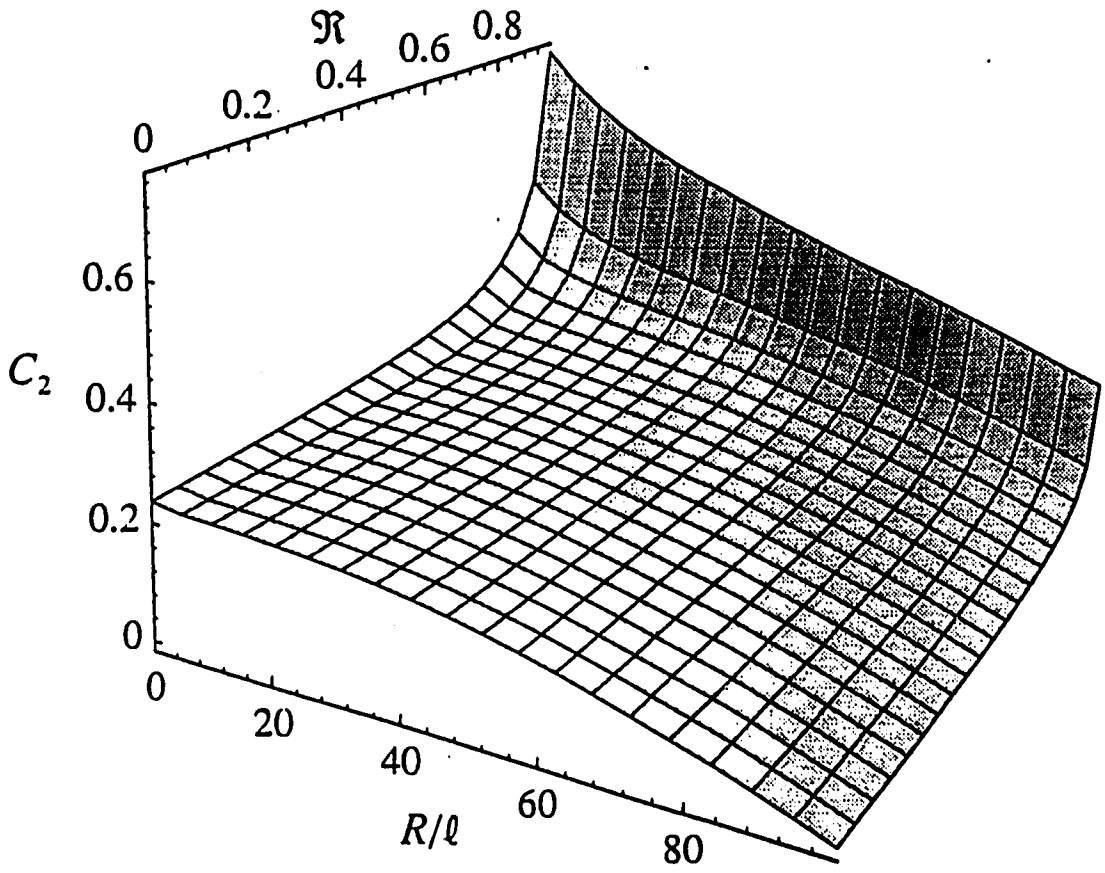

Figure 3.2

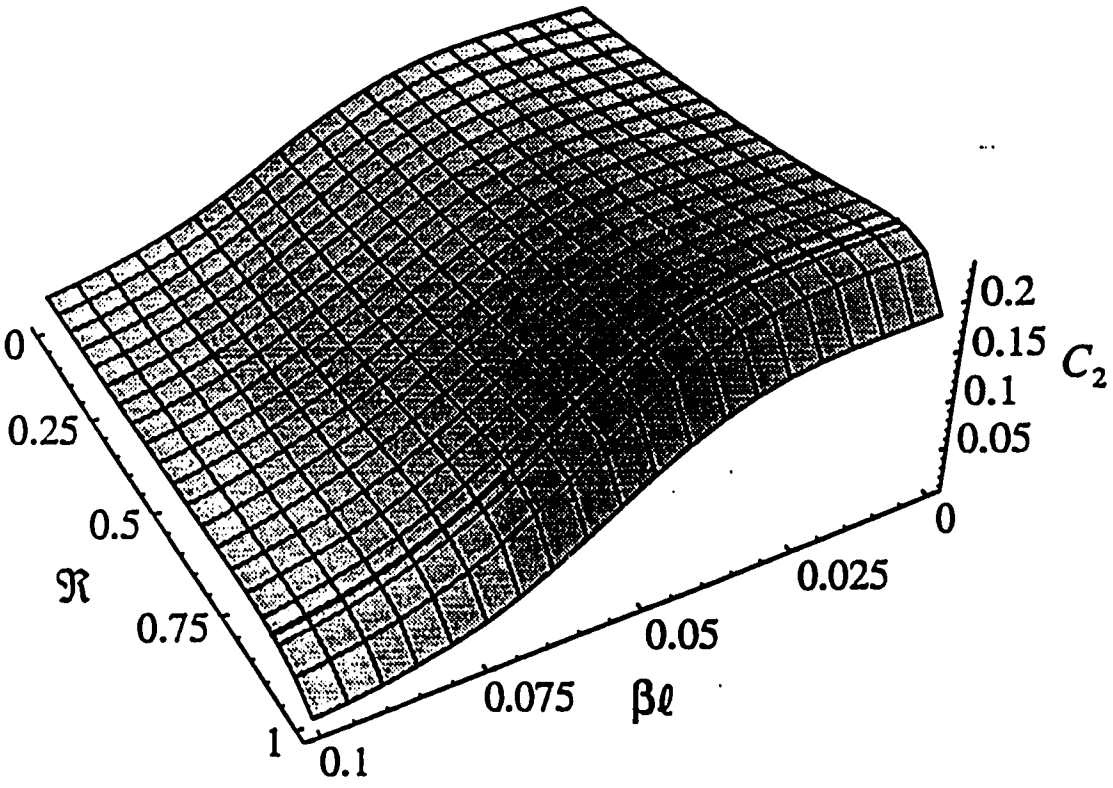

Figure 3.3

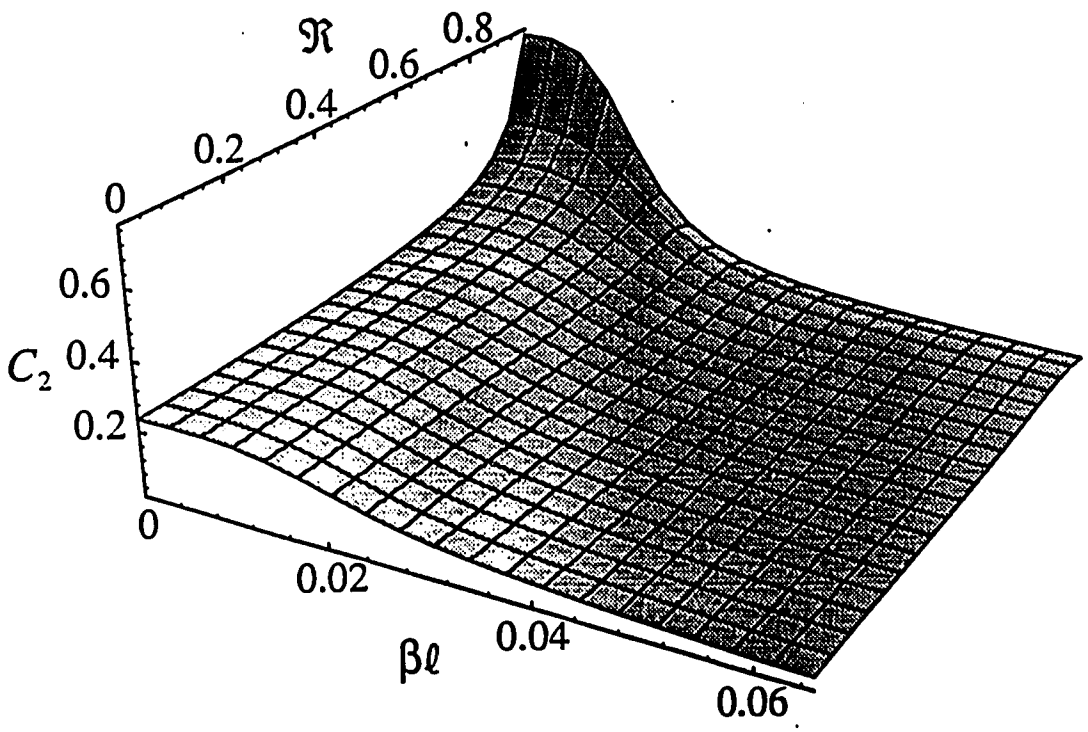

Figure 3.4

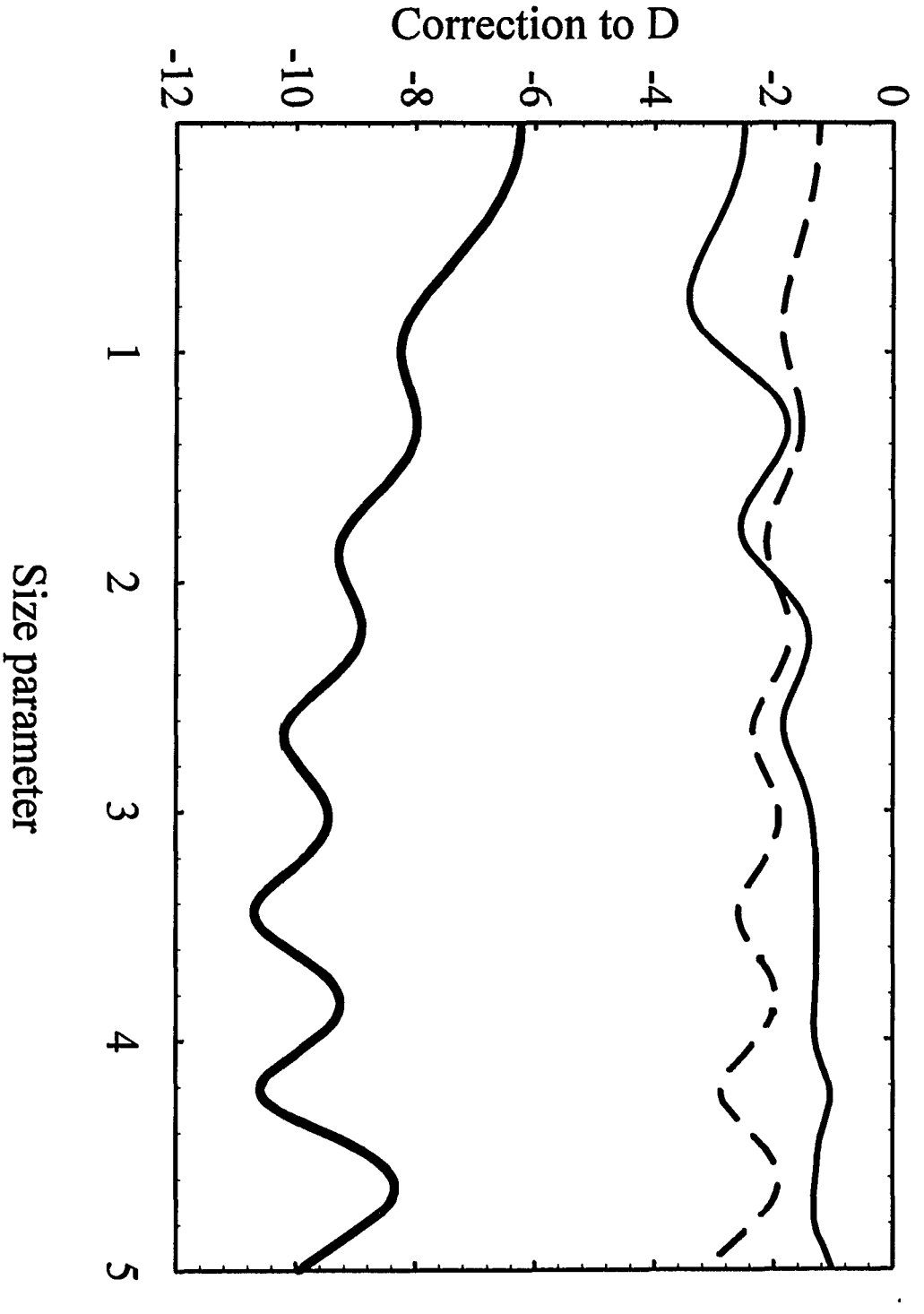

Figure 4.1

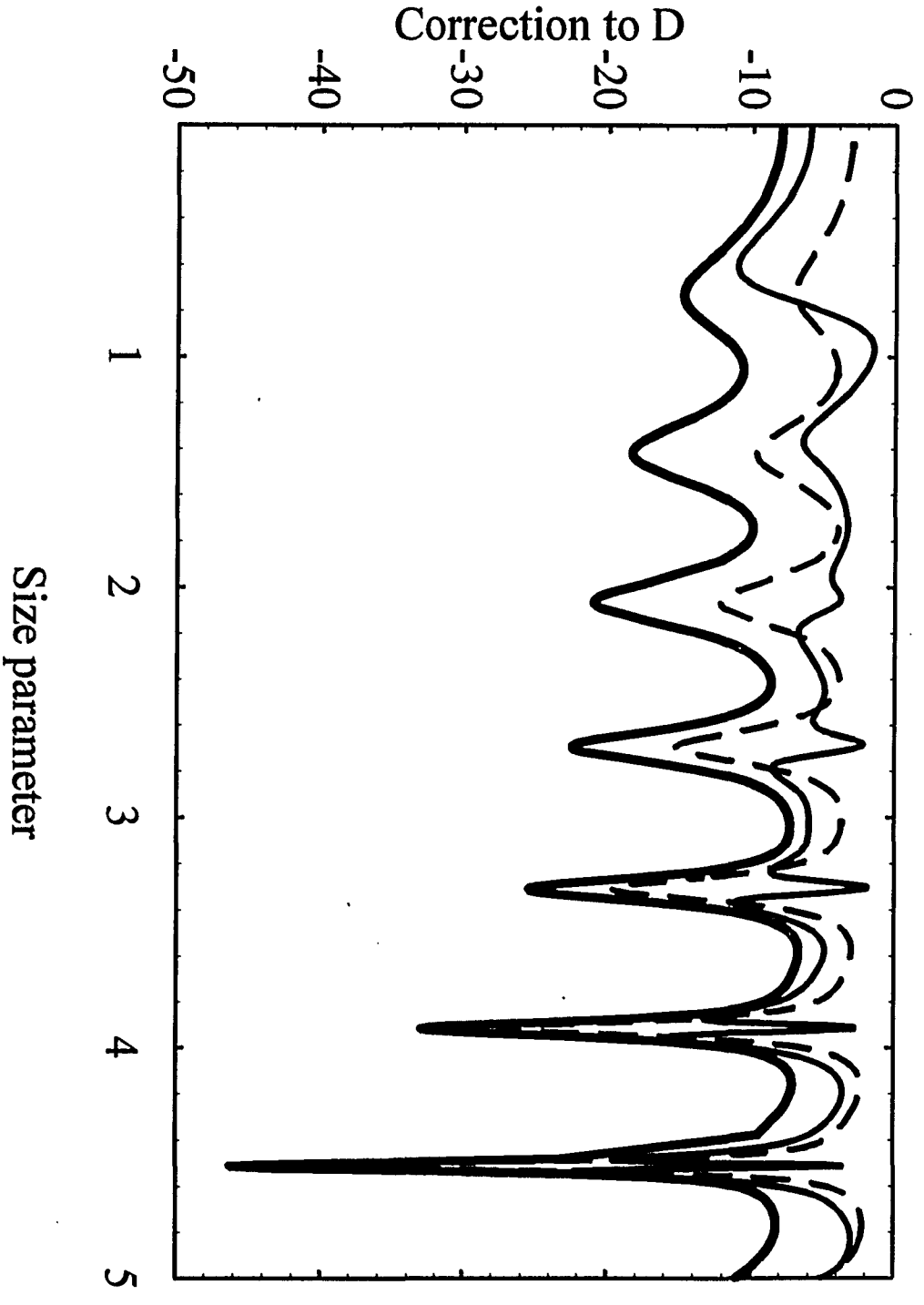

Figure 4.2

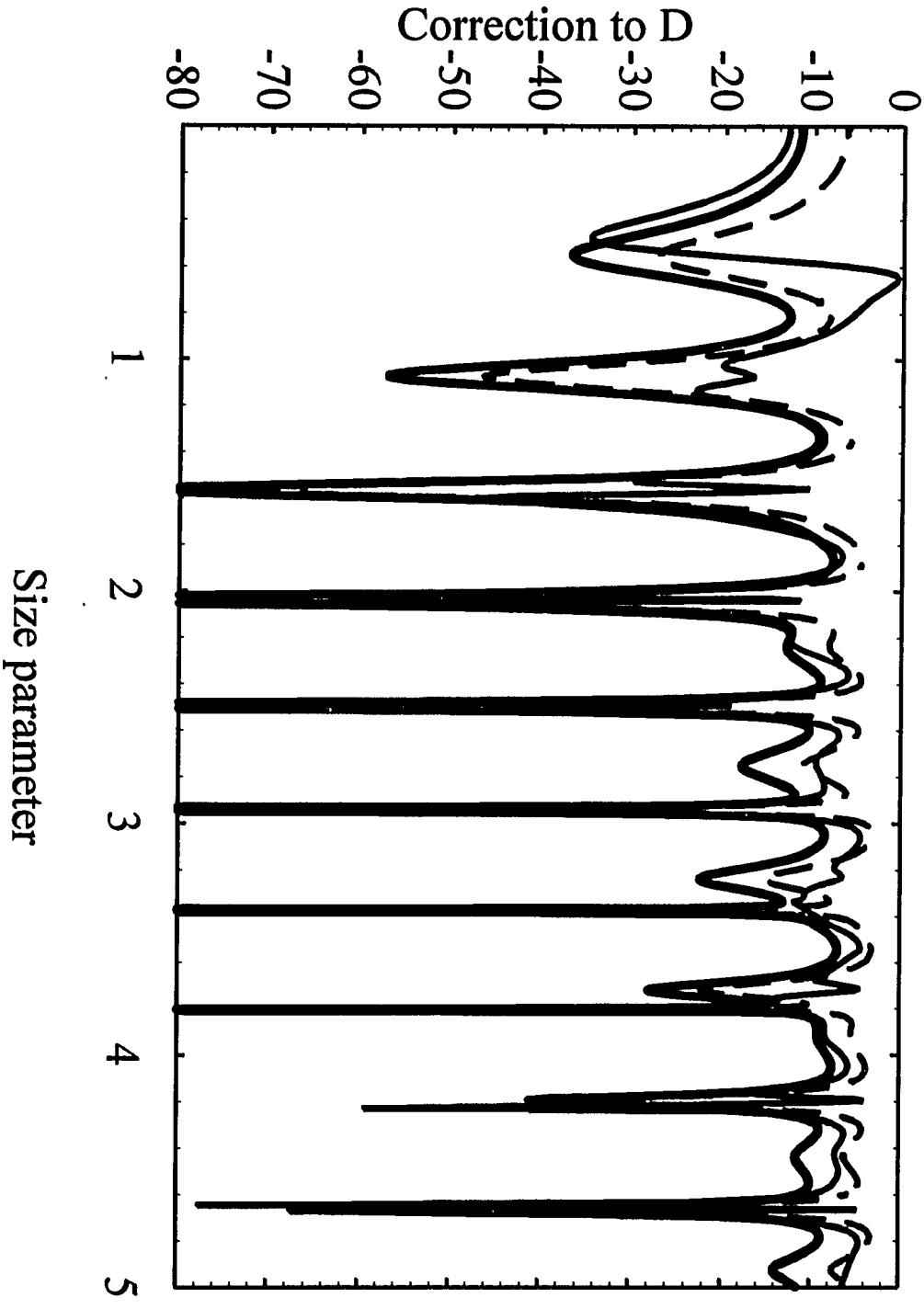

Figure 4.3

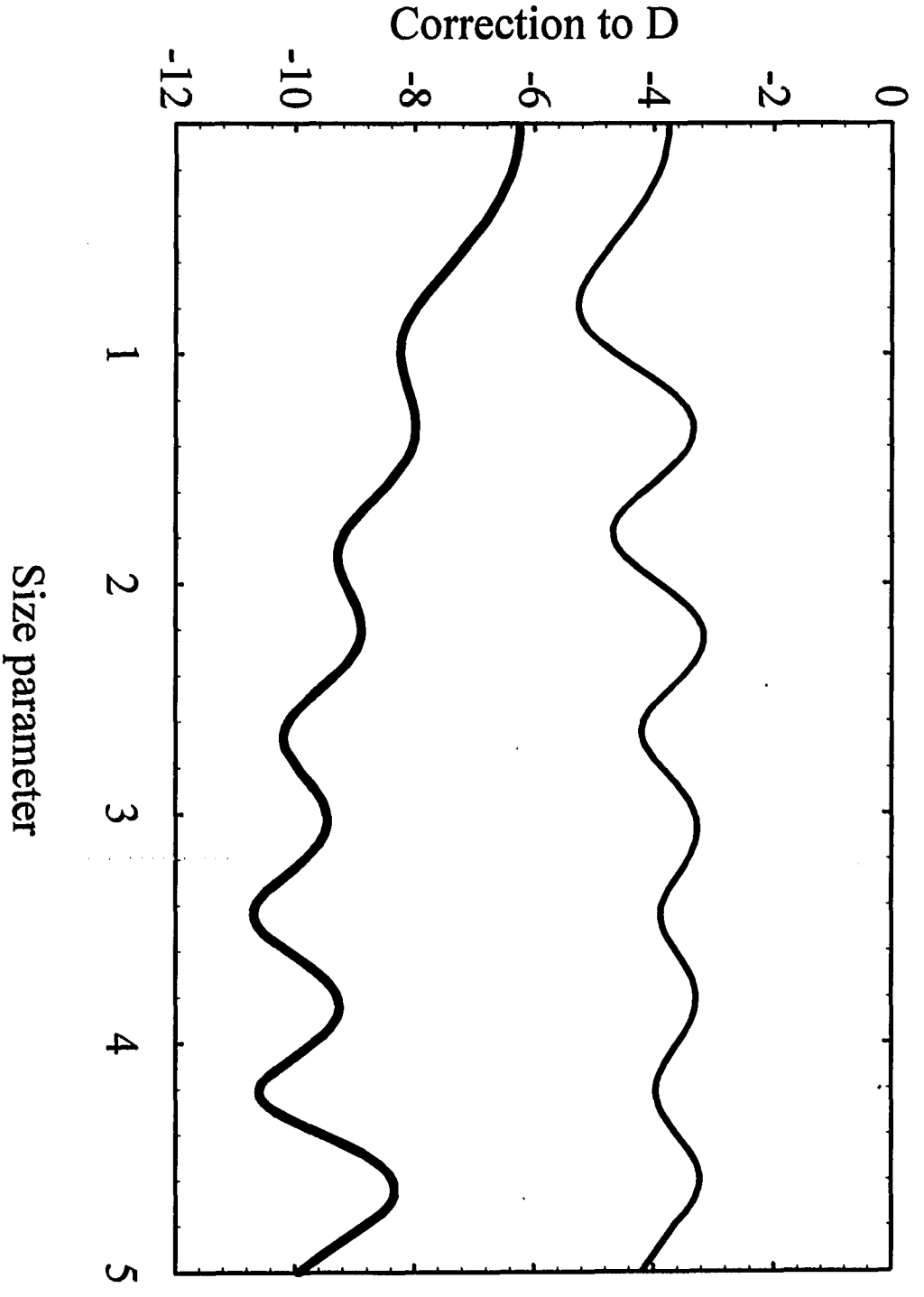

Figure 4.4

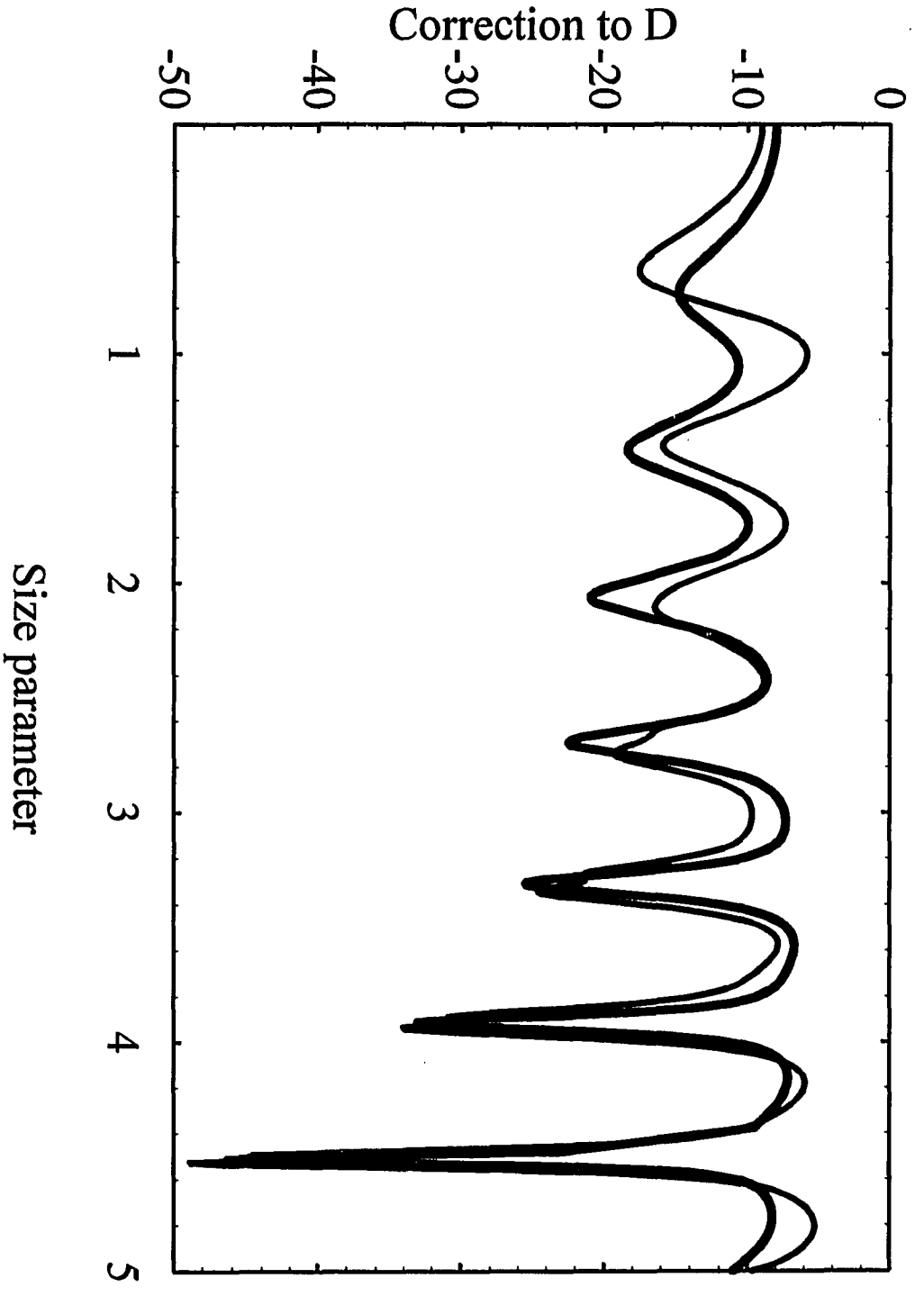

Figure 4.5

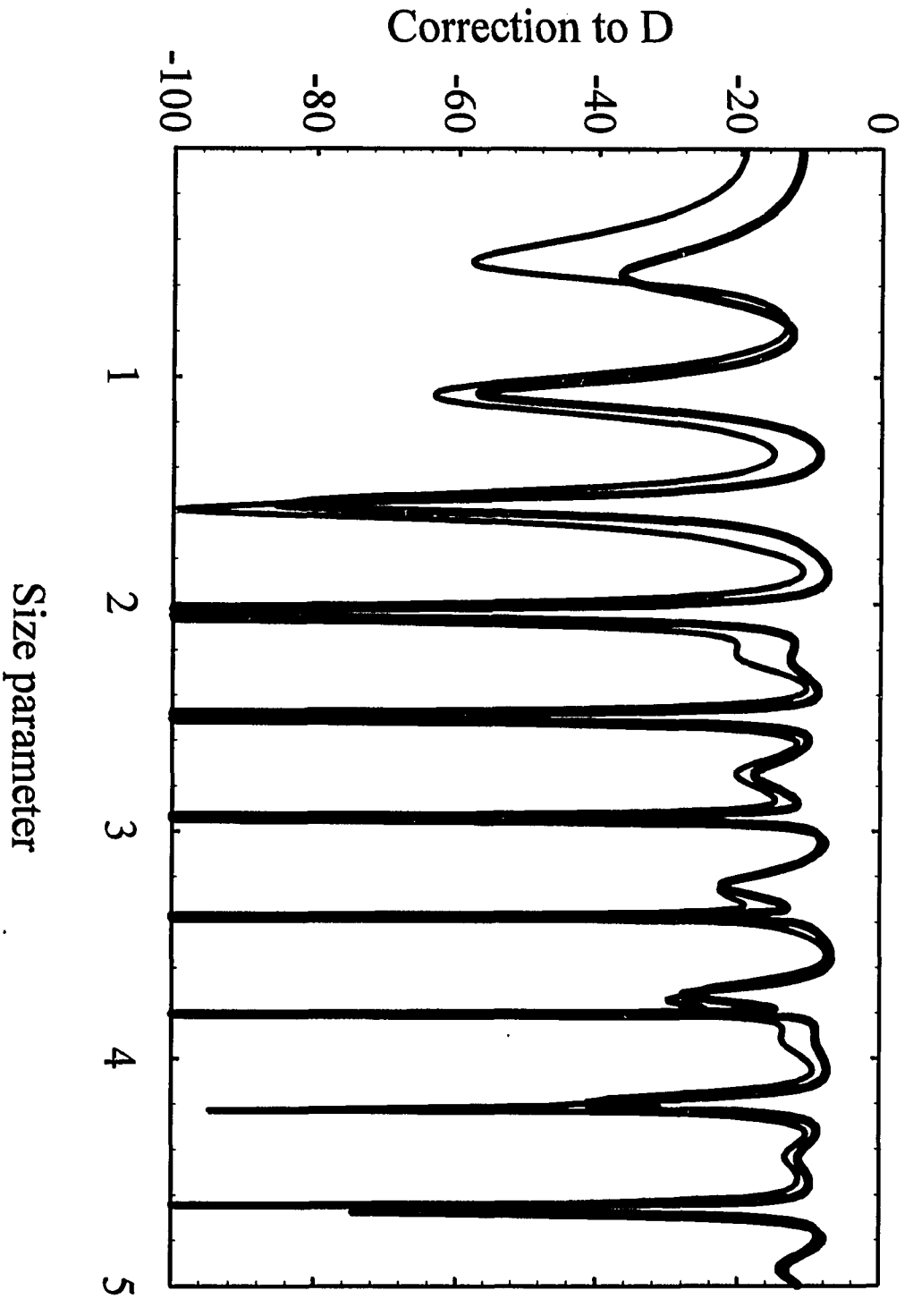

Figure 4.6

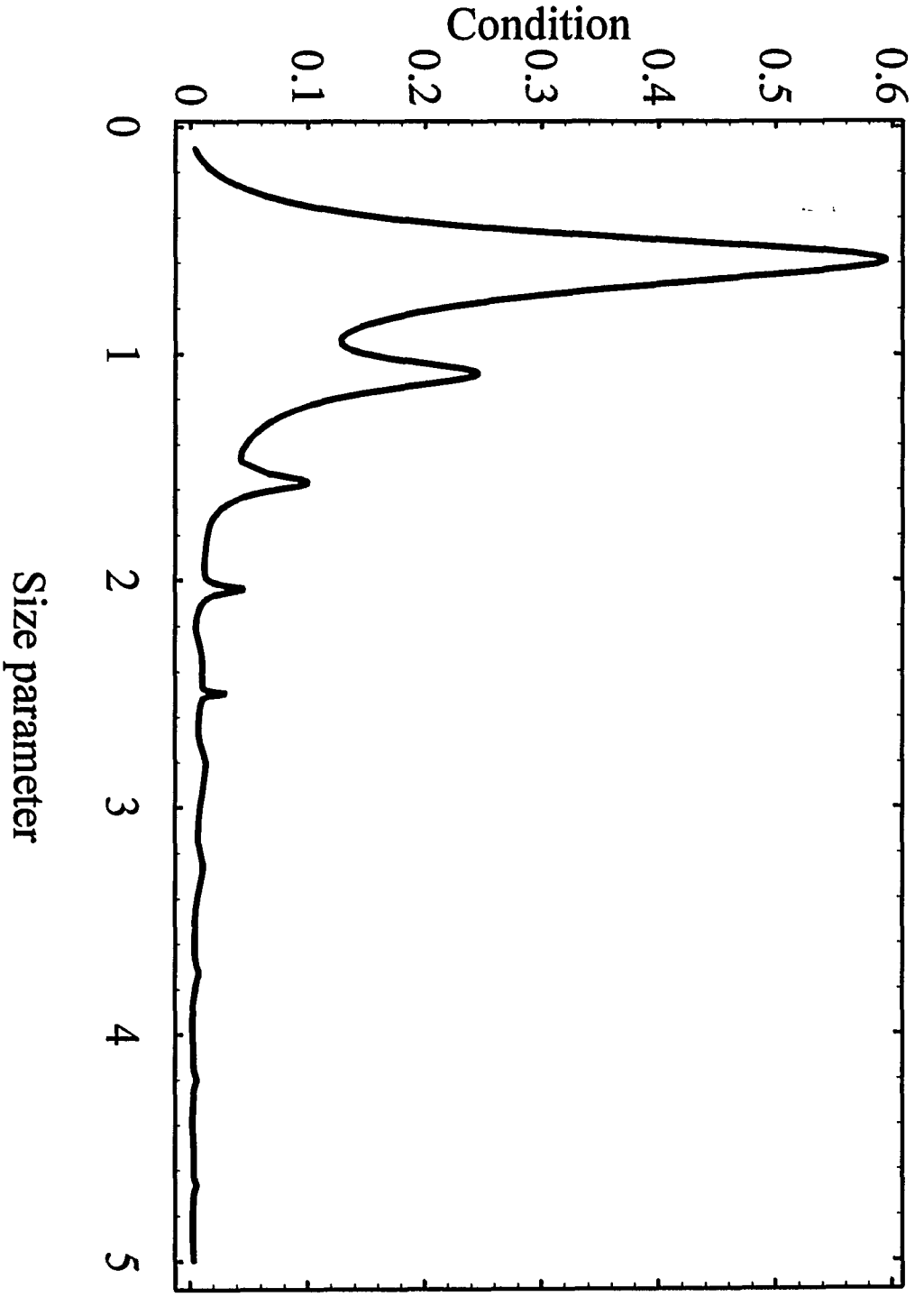

Figure 4.7

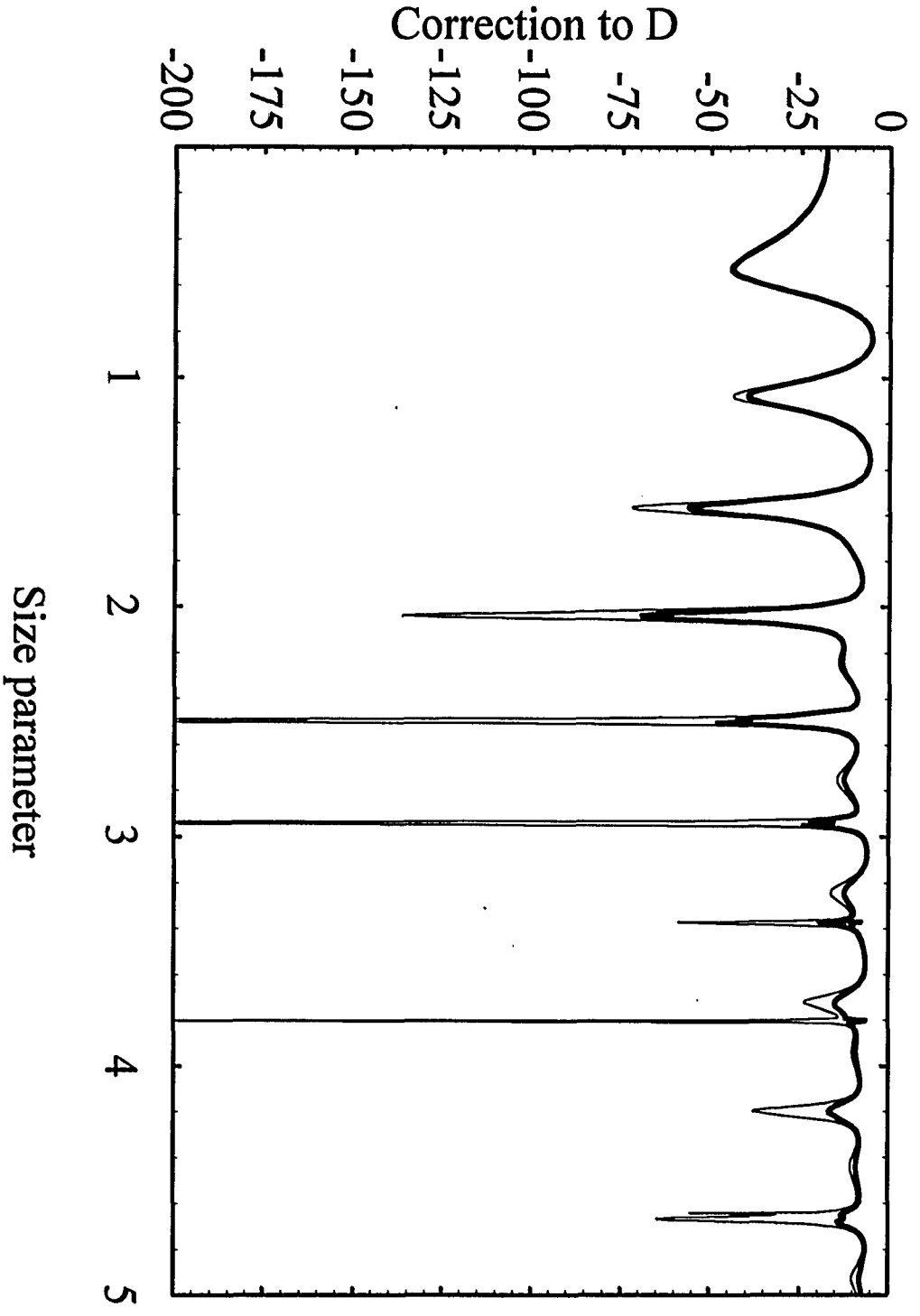
Correction to D
-200
-175
-150
-125
-100
-75
-50
-25
0
1
2
3
4
5
Size parameter

Figure 4.8

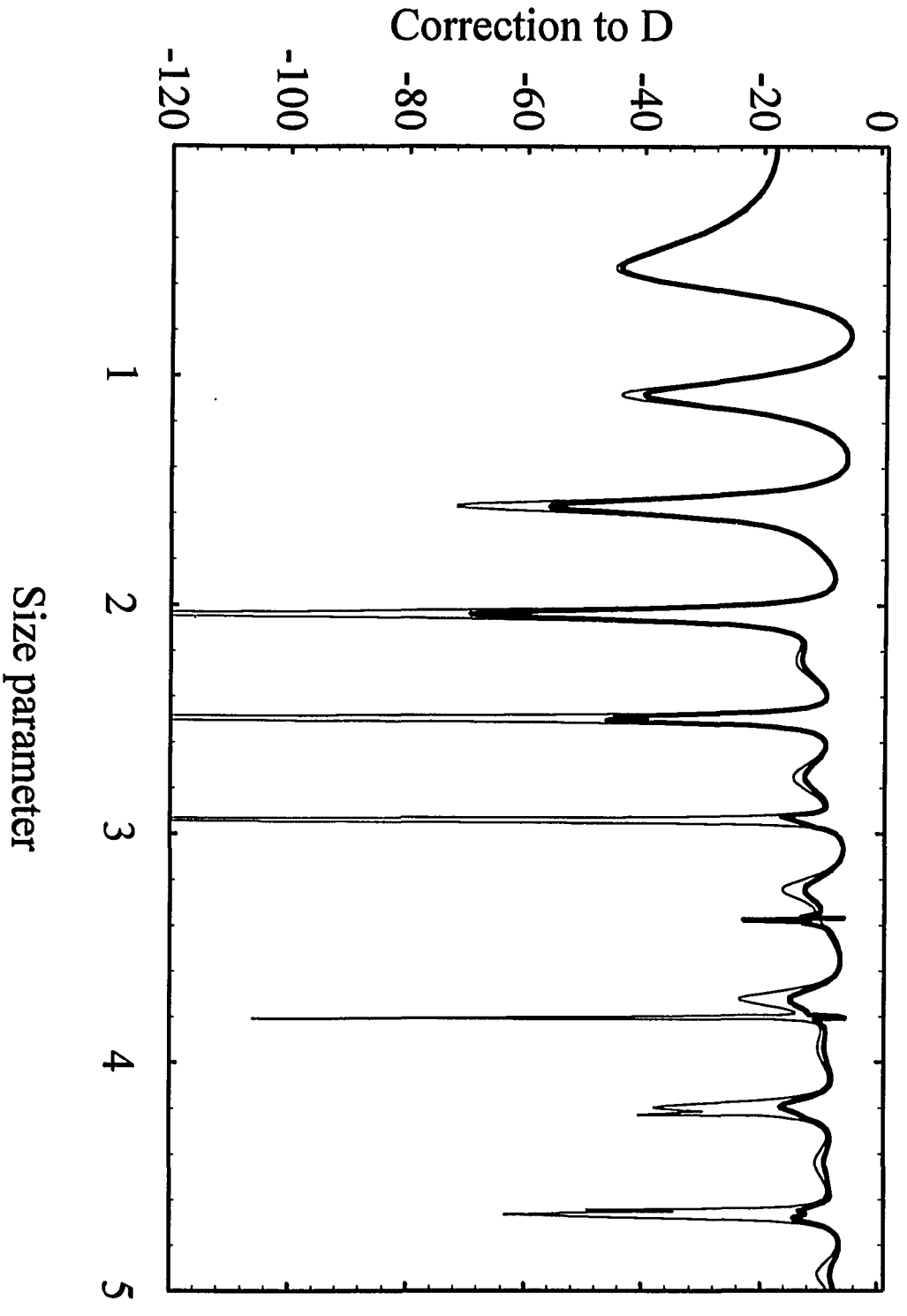

Figure 4.9

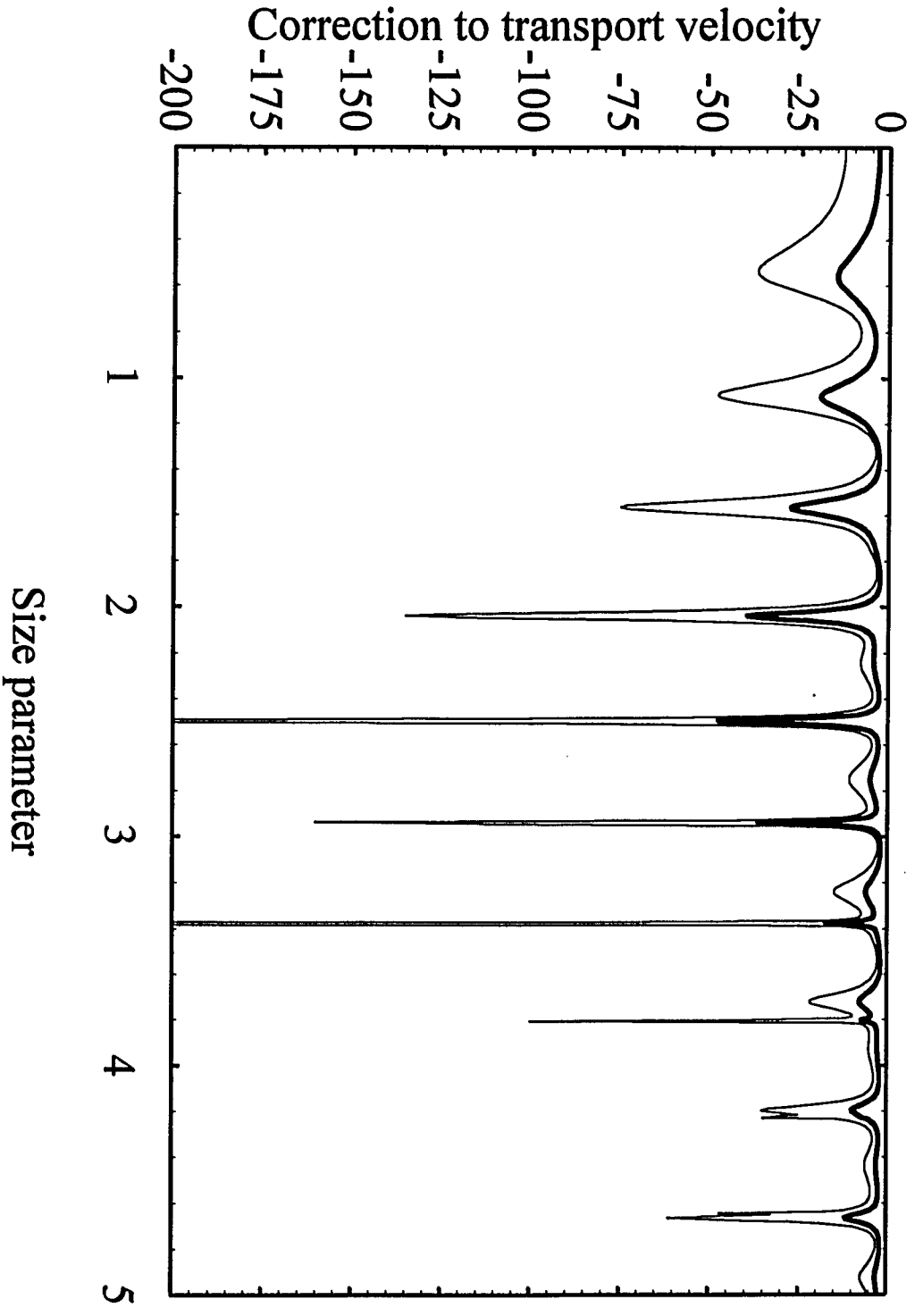
Correction to transport velocity
-200
-175
-150
-125
-100
-75
-50
-25
0
1
2
3
4
5
Size parameter

Figure 4.10

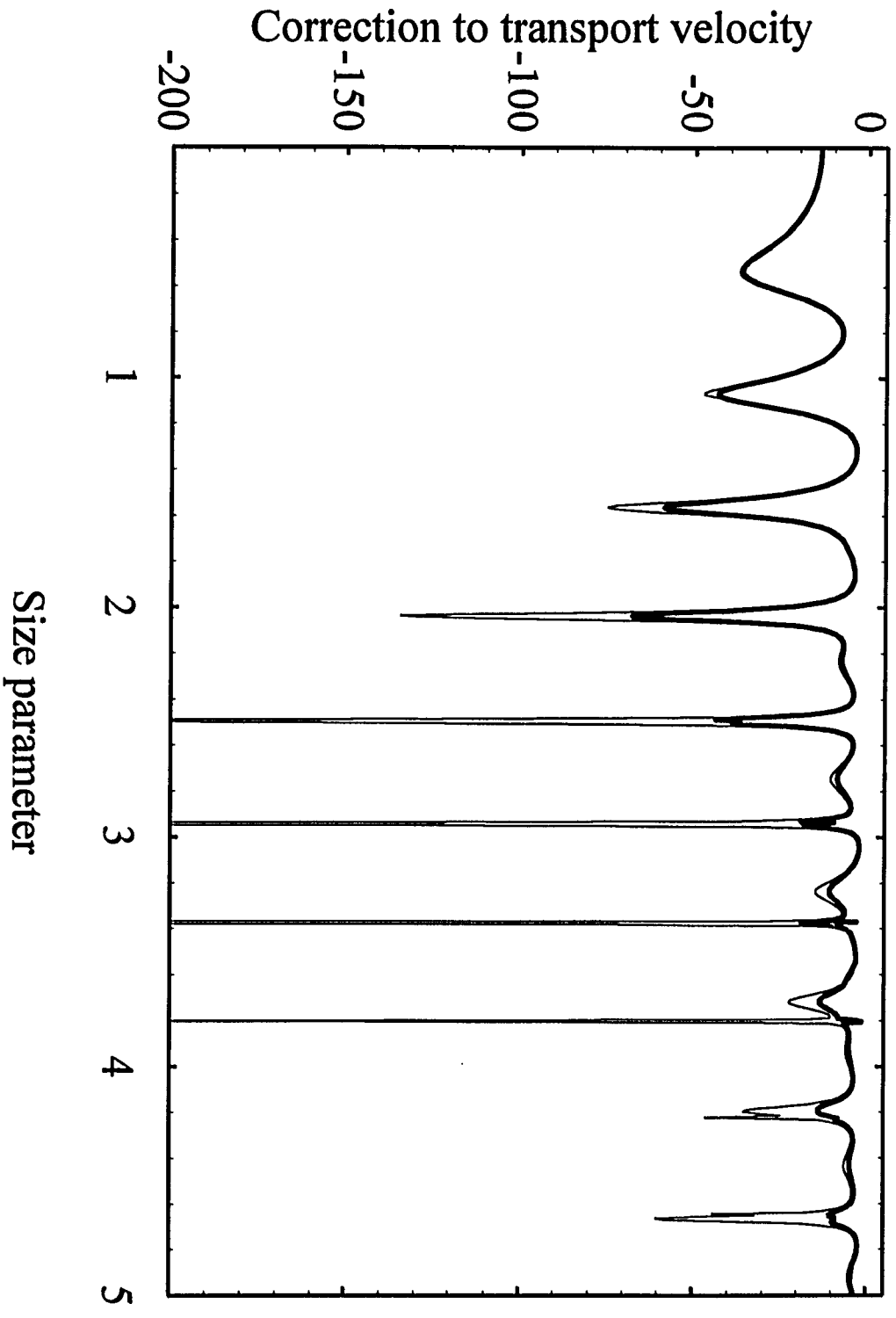
Correction to transport velocity
-200
-150
-100
-50
0
1
2
3
4
5
Size parameter

Figure 4.11

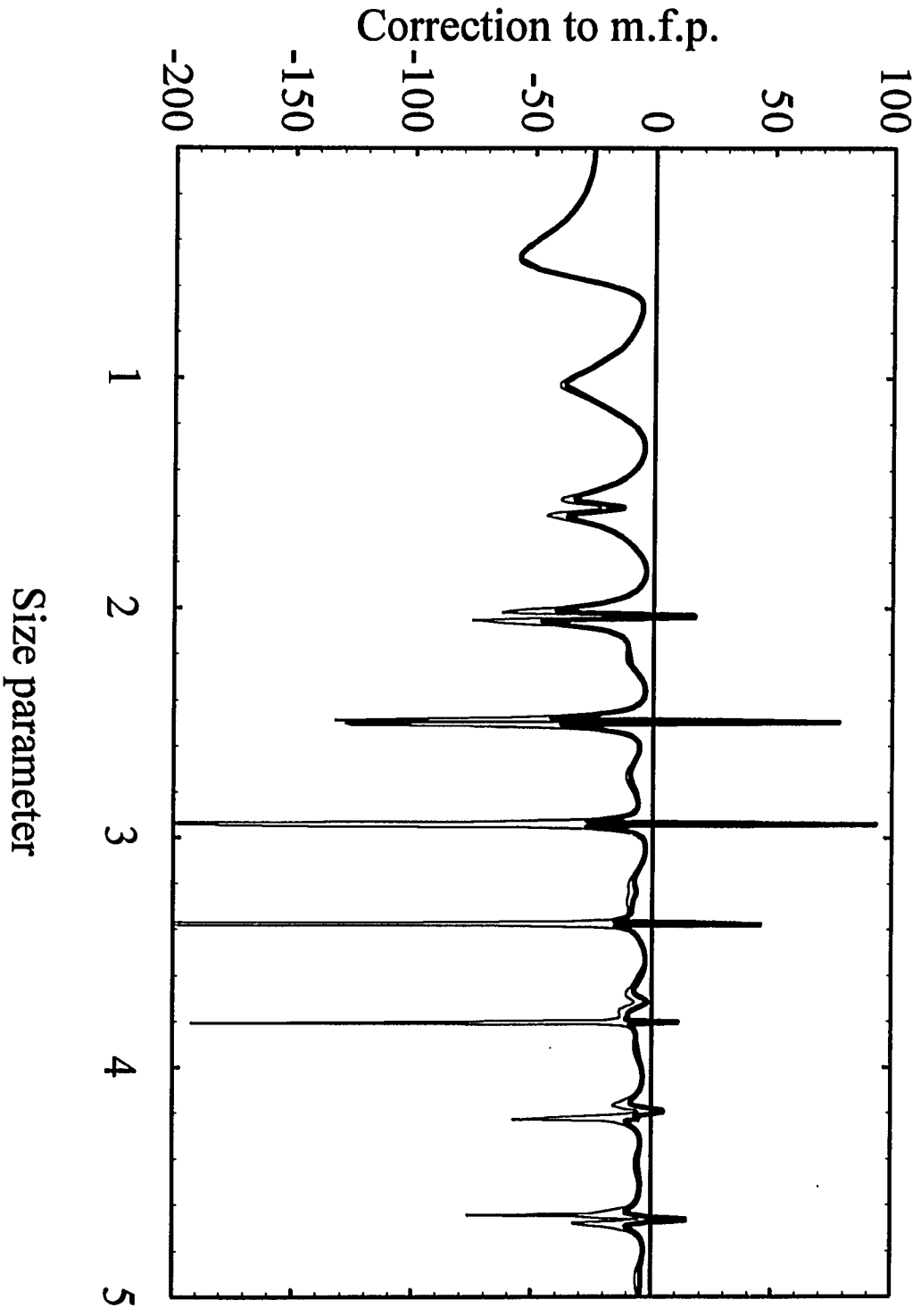
Correction to m.f.p.
-200
-150
-100
-50
0
50
100
1
2
3
4
5
Size parameter

Figure 4.12

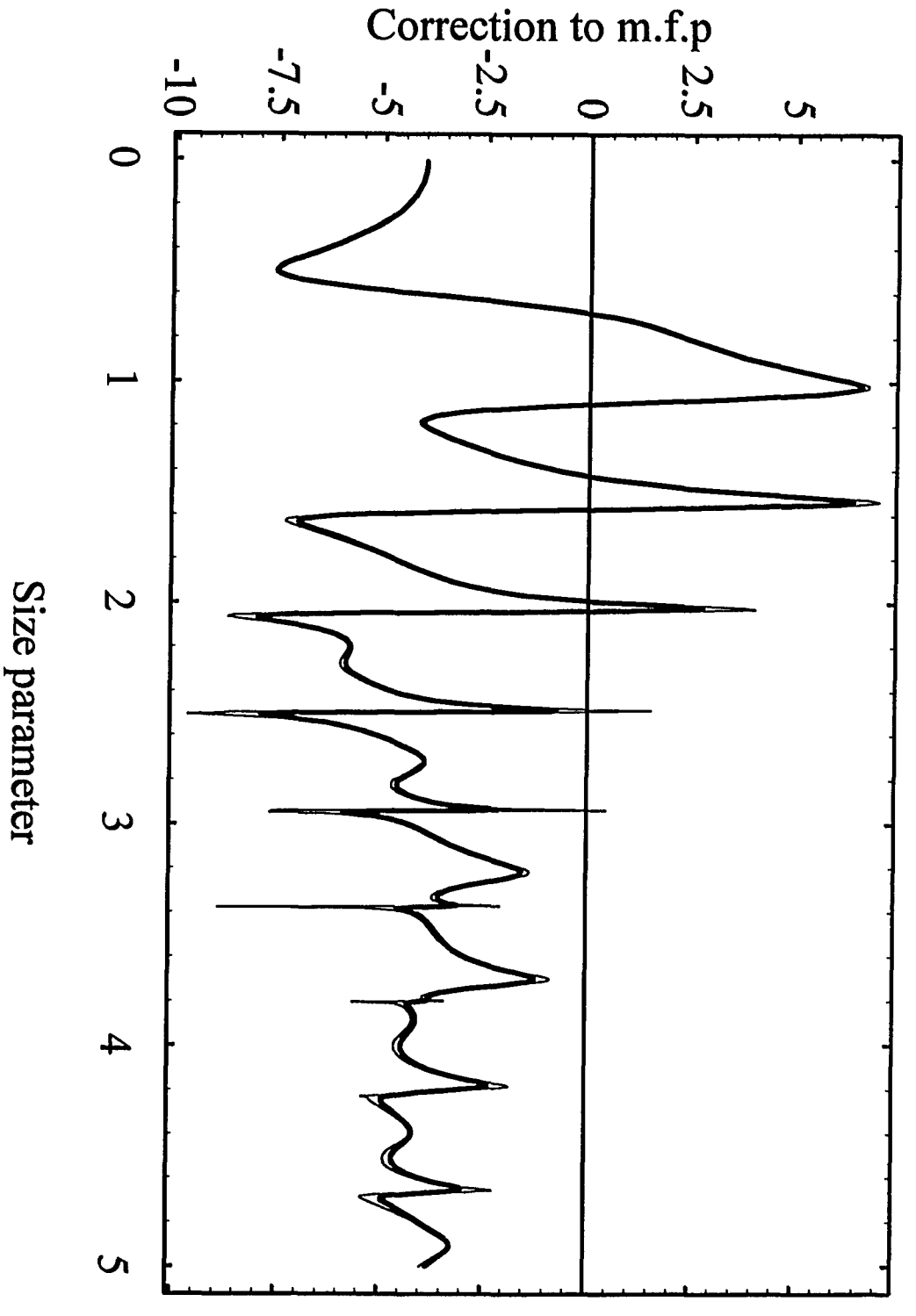

Figure 4.13

VI. APPENDIX

Here we give definitions of functions $K(x)$, $I_i(x)$ and $J_i(x)$ appearing in Eq. (3.21),

$$K(\omega) = k^2 \ell A P^2_{\omega=0}(z_p)\Big\{\Big[(1+\alpha^2 z_0^2)^2 + 4\beta^4 z_0^4\Big]\big[\cosh(2\gamma_+ L) - \cos(2\gamma_- L)\big] + 4(\gamma_+^2 + \gamma_-^2) z_0^2\big[\cosh(2\gamma_+ L) + \cos(2\gamma_- L)\big] + 4\Big[\gamma_+ z_0(1+\alpha^2 z_0^2) + 2\beta^2 \gamma_- z_0^3\Big]\sinh(2\gamma_+ L) + 4\Big[\gamma_- z_0(1+\alpha^2 z_0^2) - 2\beta^2 \gamma_+ z_0^3\Big]\sin(2\gamma_- L)\Big\} \tag{A1}$$

$$I_1(x) = \Big[1 + (\gamma_+^2 + \gamma_-^2) z_0^2\Big]\Big\{(1-\alpha^2 z_0^2)\frac{\sinh(2\gamma_+ x)}{2\gamma_+} + \frac{1}{4}(1+\alpha^2 z_0^2)\Big[\frac{\sinh[2(\gamma_+ + \alpha)x]}{\gamma_+ + \alpha} + \frac{\sinh[2(\gamma_+ - \alpha)x]}{\gamma_+ - \alpha}\Big] + \alpha z_0\Big[\frac{\sinh^2[(\gamma_+ + \alpha)x]}{\gamma_+ + \alpha} - \frac{\sinh^2[(\gamma_+ - \alpha)x]}{\gamma_+ - \alpha}\Big]\Big\}; \tag{A2}$$

$$I_2(x) = 2\gamma_+ z_0\Big\{(1-\alpha^2 z_0^2)\frac{\sinh^2(\gamma_+ x)}{\gamma_+} + \frac{1}{2}(1+\alpha^2 z_0^2)\Big[\frac{\sinh^2[(\gamma_+ + \alpha)x]}{\gamma_+ + \alpha} + \frac{\sinh^2[(\gamma_+ - \alpha)x]}{\gamma_+ - \alpha}\Big] + \frac{1}{2}\alpha z_0\Big[\frac{\sinh[2(\gamma_+ + \alpha)x]}{\gamma_+ + \alpha} - \frac{\sinh[2(\gamma_+ - \alpha)x]}{\gamma_+ - \alpha}\Big]\Big\}; \tag{A3}$$

$$I_3(x)=\left[1+(\gamma_+^2+\gamma_-^2)z_0^2\right]\left\{(1-\alpha^2z_0^2)\frac{\sinh(2\gamma_+x)}{2\gamma_+}\right.$$
$$+\frac{1}{4}(1+\alpha^2z_0^2)\left[\frac{\sinh[2(\gamma_++\alpha)x-2\alpha L]}{\gamma_++\alpha}+\frac{\sinh[2(\gamma_+-\alpha)x+2\alpha L]}{\gamma_+-\alpha}\right] \qquad \text{(A4)}$$
$$\left.-\frac{1}{2}\alpha z_0\left[\frac{\cosh[2(\gamma_++\alpha)x-2\alpha L]}{\gamma_++\alpha}-\frac{\cosh[2(\gamma_+-\alpha)x+2\alpha L]}{\gamma_+-\alpha}\right]\right\};$$

$$I_4(x)=2\gamma_+z_0\left\{(1-\alpha^2z_0^2)\frac{\sinh^2(\gamma_+x)}{\gamma_+}+\frac{1}{4}(1+\alpha^2z_0^2)\left[\frac{\cosh[2(\gamma_++\alpha)x-2\alpha L]}{\gamma_++\alpha}\right.\right.$$
$$\left.\left.+\frac{\cosh[2(\gamma_+-\alpha)x+2\alpha L]}{\gamma_+-\alpha}\right]-\frac{1}{2}\alpha z_0\left[\frac{\sinh[2(\gamma_++\alpha)x-2\alpha L]}{\gamma_++\alpha}-\frac{\sinh[2(\gamma_+-\alpha)x+2\alpha L]}{\gamma_+-\alpha}\right]\right\}; \qquad \text{(A5)}$$

$$I_5(x)=\left[1+(\gamma_+^2+\gamma_-^2)z_0^2\right]\left\{\left[(1+\alpha^2z_0^2)\cosh(\alpha L)+2\alpha z_0\sinh(\alpha L)\right]\frac{\sinh(2\gamma_+x)}{2\gamma_+}\right.$$
$$+\frac{1}{2}(1-\alpha^2z_0^2)\left[\frac{\sinh[(\gamma_++\alpha)x]\cosh[(\gamma_++\alpha)x-\alpha L]}{\gamma_++\alpha}\right. \qquad \text{(A6)}$$
$$\left.\left.+\frac{\sinh[(\gamma_+-\alpha)x]\cosh[(\gamma_++\alpha)x+\alpha L]}{\gamma_+-\alpha}\right]\right\};$$

$$I_6(x) = 2\gamma_+ z_0 \left\{ \left[(1+\alpha^2 z_0^2)\cosh(\alpha L) + 2\alpha z_0 \sinh(\alpha L) \right] \frac{\sinh(2\gamma_+ x)}{2\gamma_+} + \right.$$

$$+ \frac{1}{2}(1-\alpha^2 z_0^2) \left[\frac{\sinh[(\gamma_+ + \alpha)x]\sinh[(\gamma_+ + \alpha)x - \alpha L]}{\gamma_+ + \alpha} \right. \qquad \text{(A7)}$$

$$\left. \left. + \frac{\sinh[(\gamma_+ - \alpha)x]\sinh[(\gamma_+ + \alpha)x + \alpha L]}{\gamma_+ - \alpha} \right] \right\};$$

and functions $J_i(x)$ can be obtained from $I_i(x)$ by substitution γ_+ to $-i\gamma_-$.

IV. REFERENCES

1. P.M. Morse, H. Feshbach, *Methods of Theoretical Physics* (McGraw-Hill, NY 1953).
2. A. Ishimaru, *Wave propagation and scattering in random media* (Academic, NY 1978).
3. S. Glasstone and M.C. Edlund, *The Elements of Nuclear Reactor Theory* (Van Nostrand, New York, 1952).
4. A. Lagendijk, R. Vreeker and P. de Vries, Phys. Lett. A **136**, 81 (1989).
5. I. Freund, M. Rosenbluh and R. Berkovits, Phys. Rev. B **39**, 12403 (1989).
6. I. Freund and R. Berkovits, Phys. Rev. B **41**, 496 (1990).
7. N. Garcia, J.H. Li, W. Polkosnik, T.D. Cheung, P.H. Tsang, A.A. Lisyansky, and A.Z. Genack, Physica B **175**, 9 (1991).
8. J.X. Zhu, D.J. Pine, and D.A. Weitz, Phys. Rev. A **44**, 3948 (1991).
9. P.M. Saulnier and G.H. Watson, Optics Lett. **17**, 946 (1992).
10. N. Garcia, A.Z. Genack, and A.A. Lisyansky, Phys. Rev. B **46**, 14475 (1992).
11. J.H. Li, A.A. Lisyansky, T.D. Cheung, D. Livdan, and A.Z. Genack, Europhys. Lett. **22**, (1993) 675.
12. A.A. Lisyansky, J.H. Li, D. Livdan, N. Garcia, T.D. Cheung, and A.Z. Genack, in Photonic Band Gaps and Localization, C.M. Soukoulis, ed., (Plenum Press, New York, 1993), p. 171.
13. A.A. Lisyansky, D. Livdan, J.H. Li, T.D. Cheung, and A.Z. Genack, in OSA

Proceedings on Advances in Optical Imaging and Photon Migration ('94)

14. A.Z. Genack, Phys. Rev. Lett **58**, 2043 (1987).

15. I. Freund, M. Rosenbluh, and S. Feng, Phys. Rev. Lett. **61**, 2328 (1988).

16. N. Garcia and A.Z. Genack, Phys. Rev. Lett. **63**, 1678 (1989).

17. A.Z. Genack and J. M. Drake, Europhys. Lett. **11**, 331 (1990).

18. A.Z. Genack, in *Classical Waves Localization*, edited by P. Sheng (World Scientific, Singapore, 1990).

19. M.P. van Albada, J.F. de Boer, and A. Lagendijk, Phys. Rev. Lett. **64**, 2787 (1990).

20. A.Z. Genack, N. Garcia, and W. Polkosnik, Phys. Rev. Lett. **65**, 2129 (1990).

21. A.Z. Genack, N. Garcia, J. Li, W. Polkosnik and J.M. Drake, Physics A **168**, 387 (1990).

22. N. Garcia and A.Z. Genack, Opt. Lett. **16**, 132 (1991).

23. J.F. de Boer, M.P. van Albada and A. Lagendijk, Phys. Rev. **45**, 658 (1992).

24. B. Shapiro, Phys. Rev. Lett **57**, 2168 (1986).

25. M.J. Stephen and G. Cwilich, Phys. Rev. Lett. **59**, 285 (1987).

26. M.J. Stephen, Phys. Lett. A **127**, 381 (1987).

27. A.Yu. Zyuzin and B.Z. Spivak, Zh. Eksp. Teor. Fiz. **93**, 994 (1987) [Sov. Phys. JETP **66**, 560 (1987)].

28. A.Yu. Zyuzin and B.Z. Spivak, Solid State Commun. **65**, 311 (1988).

29. S. Feng, C. Kane, P.A. Lee, and A.D. Stone, Phys. Rev. Lett. **61**, 834 (1988).

30. I. Edrei and M. Kaveh, Phys. Rev. B **38**, 950 (1988).

31. R. Pnini and B. Shapiro, Phys. Rev. B **39**, 6986 (1989).

32. R. Berkovits, M. Kaveh, and S. Feng, Phys. Rev. B **40**, 737 (1989).

33. I. Edrei and M. Kaveh, Phys. Rev. B **40**, 9419 (1989).

34. P. Pnini and B. Shapiro, Phys. Lett. A**157**, 265 (1991).

35. E. Kogan and M. Kaveh, Phys. Rev. **45**, 1049 (1992).

36. A.A. Lisyansky and D. Livdan, Phys. Lett. A**170**, 53 (1992).

37. A.A. Lisyansky and D. Livdan, Phys. Rev. B **47**, 14157 (1993).

38. M.P. van Albada, B.A. van Tiggelen, A. Lagendijk, and A. Tip, Phys. Rev. Lett. **62**, 3132 (1991).

39. B.A. van Tiggelen, A. Lagendijk, M.P. van Albada, and A.Tip, Phys. Rev. B **45**, 12233 (1992).

40. G. Cwilich and Y. Fu, Phys. Rev. B **46**, 12015 (1992).

41. E. Kogan and M. Kaveh, Phys. Rev. B **46**, 10636 (1992).

42. Yu.N. Barabanenkov and V.D. Ozrin, Phys. Rev. Lett. **69**, 1364 (1992).

43. J. Kroha, C.M. Soukoulis and P. Wolffe, Phys. Rev. B **47**, 9208 (1992).

44. C. M. Soukoulis, S. Datta, and E. N. Economou, Phys. Rev. B **49**, 3800-3804 (1993).

45. B.A. van Tiggelen and A. Lagendijk, Europhys. Lett. **23**, 311 (1993).

46. B.A. van Tiggelen, A. Lagendijk, and A. Tip, Phys. Rev. Lett. **71**, 1284 (1993).

47. D. Livdan and A.A. Lisyansky, preprint.

48. *Mesoscopic Phenomena in Solids*, edited by B.L. Altshuler, P.A. Lee, and

R.A. Webb (Elsevier Science, 1991).

49. S. John, Phys. Today **44** (5), 32 (1991).

50. Scattering and Localization of Classical Waves in Random Media, ed. by Ping Sheng (World Scientific, Singapore, 1990).

51. Z.Q. Zhang and P. Sheng, in Scattering and Localization of Classical Waves in Random Media, ed. Ping Sheng (World Scientific, Singapore, 1990), pp. 137-178.

52. E.P. Wigner, Phys. Rev. **98**, 145 (1955).

53. G. Mie, Ann. Physik, **25**, 377 (1908).

54. P.W. Anderson, Phil. Mag. B **52**, 505 (1985).

55. D. Vollhard and P. Wolfle, Phys. Rev. B **22**, 4666 (1980).

56. Yu.N. Barabanenkov and V.D. Ozrin, Phys. Lett. A **154**, 38 (1991).

57. A.Z. Genack, J.H. Li, N. Garcia and A.A. Lisyansky, in Photonic Band Gaps and Localization, ed. C.M. Soukoulis (Plenum Press, New York, 1993), pp.23-55.

58. H.C. van de Hulst, Light Scattering by Small Particles (Wiley, New York, 1957).

59. M. Goldberg and K. Watson, Collision Theory (Wiley, New York, 1964), p. 750.

60. T.R. Kirkpatrick and J.R. Dorfman, in Statistical Physics VI, ed. E.G.D. Cohen (North-Holland, Amsterdam, 1985).

61. M. Kaveh and E. Kogan, in Photonic Band Gaps and Localization, C.M. Soukoulis, ed., (Plenum Press, New York, 1993), pp. 187 - 194.

62. Yu.N. Barabanenkov, Izv. Vyssh. Uchebn. Zaved. Radiofiz. **11**, 720 (1968).

63. M. Lax, Rev. Mod. Phys. **23**, 287 (1951).

64. P. Lloyd, J. Phys. C **2**, 1717 (1968).